DR. ADAM MILLER (Orcid ID : 0000-0002-1632-7206)
DR. COLLIN W AHRENS (Orcid ID : 0000-0002-0614-9928)

Article type : Original Article

Local and regional scale habitat heterogeneity contribute to genetic adaptation in a commercially important marine mollusc (*Haliotis rubra*) from southeastern Australia

A. D. Miller[1,2*], A. A. Hoffmann[3], M. H. Tan[1,2], M. Young[1], C. Ahrens[4], M. Cocomazzo[1], A. Rattray[1], D. A. Ierodiaconou[1], E. Treml[1], C. D. H Sherman[1,2]

[1] Deakin University, Geelong, School of Life and Environmental Sciences, Centre for Integrative Ecology, Warrnambool, Victoria, Australia

[2]Deakin Genomics Centre, Deakin University, Geelong, VIC 3220, Australia

[3] School of BioSciences, Bio21 Institute, The University of Melbourne, Parkville, Victoria, Australia

[4] Hawkesbury Institute for the Environment, Western Sydney University, Hawkesbury, New South Wales, Australia

*Corresponding author: Adam D. Miller (a.miller@deakin.edu.au)

Abstract

Characterising adaptive genetic divergence among conspecific populations is often achieved by studying genetic variation across defined environmental gradients. In marine systems this is challenging due to a paucity of information on habitat heterogeneity at local and regional scales and a dependency on sampling regimes that are typically limited to broad longitudinal and latitudinal environmental gradients. As a result, the spatial scales at which selection processes operate and the environmental factors that contribute to genetic adaptation in marine systems are likely to be unclear. In this study we explore patterns of adaptive genetic structuring in a commercially-harvested abalone species (*Haliotis rubra*) from south-eastern Australia, using a panel of genome-wide SNP markers (5,239 SNPs), and a sampling regime informed by marine LiDAR bathymetric imagery and 20-year hindcasted oceanographic models. Despite a lack of overall genetic structure across the sampling distribution, significant genotype associations with heterogeneous habitat features were observed at local and regional spatial scales, including associations with wave energy, ocean current, sea surface temperature, and geology. These findings provide insights into the potential resilience of the species to changing marine climates and the role of migration and selection on recruitment processes, with implications for conservation and fisheries management. This study points to the spatial scales at which selection processes operate in marine systems and highlights the benefits of geospatially-informed sampling regimes for overcoming limitations associated with marine population genomic research.

Keywords: abalone, population genomics, genetic adaptation, environmental heterogeneity, LiDAR, hindcasted oceanographic models, fisheries management, marine conservation

Introduction

Modern genomic approaches have revolutionized the field of population genetics, providing unprecedented sensitivity for resolving patterns of genetic variation between individuals and populations (Davey *et al.* 2011; Ekblom & Galindo 2011). Notably, these technologies help characterise patterns of adaptive genetic diversity among conspecific populations (Stapley *et al.* 2010; Savolainen *et al.* 2013). Reduced genome representation, whole genome, and transcriptome sequencing approaches are being used routinely for describing signatures of selection and

identifying putative candidate genes that underlie adaptive differences between species populations (Stapley *et al.* 2010; Ahrens *et al.* 2018). Studies of this nature ideally require sampling regimes that allow genetic variation to be contrasted among conspecific populations distributed across defined environmental gradients (Frichot *et al.* 2013). Most have been carried out in terrestrial systems where habitat heterogeneity is relatively easy to measure and is often well described, with many demonstrating evidence of selection resulting from environmental variation at various spatial scales (Buehler *et al.* 2013; Jordan *et al.* 2017; Termignoni-Garcia *et al.* 2017; Pfeifer *et al.* 2018). In contrast, information on the heterogeneity of marine habitats, particularly benthic habitats, is limited for many coastlines, hindering effective sampling to test for adaptive genetic diversity within marine species. Instead, sampling regimes for marine studies are typically limited to broad-scale environmental gradients (Nielsen *et al.* 2009; Hess *et al.* 2013; Milano *et al.* 2014), and tend to overlook habitat variation at local scales. As a result, the spatial scales at which selection processes operate and the environmental factors that contribute to genetic adaptation in marine systems can be unclear.

Advances in marine geospatial science offer new opportunities for overcoming these limitations (Grummer *et al.* 2019). LiDAR and SONAR technologies are being increasingly used for imaging seabeds around the world and characterising the complexity and connectivity of benthic marine habitats (Brown *et al.* 2011; Ierodiaconou *et al.* 2011; Lecours *et al.* 2015; Young *et al.* 2016) (Figure S3). These types of datasets are important for marine navigation, ecological research, and conservation and fisheries management (Pickrill & Todd 2003; Brock & Purkis 2009; Cogan *et al.* 2009), and as a result, a variety of international and national seafloor mapping projects have been initiated in recent years. These include the GEBCO Seabed 2030 Project which has an ambitious target of mapping the world ocean by 2030 (Mayer *et al.* 2018). In addition to information on the benthic structure of the seafloor, an understanding of the dynamic nature of the physical marine environment is being enhanced by contemporary and hindcasted models of physical oceanographic variables (e.g. hydrodynamics and sea surface temperature) for coastal and offshore marine environments around the world (Burrows *et al.* 2011; Young *et al.* 2011; Hemer *et al.* 2013). The integration of physical oceanographic models with seafloor maps can be used to effectively quantify habitat heterogeneity across marine systems. In turn, there is an opportunity to overcome sampling constraints associated with marine population genomic research, and to develop efficient strategies to quantify genetic diversity across environmental gradients (Grummer *et al.* 2019).

Understanding patterns of contemporary genetic structure and the presence of standing genetic variation for adaptation to changing environmental conditions helps direct effective management approaches for threatened, invasive and commercially important marine species (Hoffmann & Sgro 2011; Weeks *et al.* 2017; Miller *et al.* 2018). In particular, research geared toward assessing the extent of genetic structure across broad geographical gradients, and genetic

variation available for adaptation to more acidic and higher temperature environments, can quantify the resilience of marine species under climate change (Hoegh-Guldberg & Bruno 2010; Torda *et al.* 2017; Miller *et al.* 2018). Additionally, adaptive genetic divergences among populations, particularly on finer spatial scales, can assist in deciphering the influence of natural selection on recruitment processes (Marshall *et al.* 2010). Studies on marine fish and invertebrates have demonstrated that adaptive variation can be maintained despite high levels of gene flow (Galindo *et al.* 2009; Martinez-Fernandez *et al.* 2010; Hess *et al.* 2013; Solas *et al.* 2013; Milano *et al.* 2014; Sandoval-Castillo *et al.* 2018), suggesting that selection can influence recruitment processes as some potential recruits are expected to be maladapted to certain habitat types (Marshall *et al.* 2010). Information on gene flow and population connectivity informs whether populations can replenish naturally following disturbance and depletion, and when management intervention is required (Whiterod *et al.* 2017). To assist intervention activities, such as translocations and reseeding, information on neutral and adaptive genetic differentiation among populations is needed to help identify environmentally compatible genotypes (Ward 2006; Weeks *et al.* 2011). This is pertinent to commercial fisheries (Hauser & Carvalho 2008; Waples *et al.* 2008), where stock augmentation activities are being adopted to assist recovery after depletion (Bell *et al.* 2005; Roodt-Wilding 2007).

Abalone are a group of marine benthic molluscs belonging to the family Haliotidae that are targeted commercially in eleven countries, forming an important global industry worth approximately $US180 million annually (Gordon & Cook 2013). In recent decades many abalone fisheries have collapsed due to over-exploitation, extreme weather events, environmental change and disease, with a number of target species now listed as endangered or considered ‘species of concern’ (Leiva & Castilla 2001; Gruenthal & Burton 2005; Kashiwada & Taniguchi 2007). Current management of abalone fisheries assumes limited connectivity, with stock viability dictated by recruitment from local sources. This assumption is based on ecological studies suggesting that the planktonic larval dispersal is limited for many abalone species (Hahn 1988; Prince *et al.* 1987; Mcshane *et al.* 1988; Prince *et al.* 1988). However, genetic studies of various Haliotids indicate conflicting patterns of population connectivity and genetic structure (Chambers *et al.* 2006; Gruenthal *et al.* 2007; Gruenthal & Burton 2008; Piggott *et al.* 2008; Miller *et al.* 2014), suggesting that larval dispersal and population connectivity are spatially and temporally variable and influenced by abiotic factors such as ocean currents and wave energy (Miller *et al.* 2016). While these studies have provided novel insights into neutral genetic structuring and population connectivity within abalone species, there is little information on adaptive genetic differentiation, the influence of selection on recruitment processes, and the likely resilience of Haliotids to environmental change.

Recent genomic analyses have revealed broad geographic patterns of putatively adaptive genetic structure in connected metapopulations of *Haliotis* species from Australia and North America. Analyses of reduced genome representation data from Western Australian greenlip abalone (*Haliotis laevigata*) provided evidence of adaptive genetic variation correlated with sea surface temperature and oxygen concentrations (Sandoval-Castillo *et al.* 2018). Genotype by environment association analyses performed by Sandoval- Castillo *et al.* (2018) revealed genetic variants under selective pressure, including variants in annotated genes with functions related to high temperature and/or low oxygen tolerances. Similarly, analyses of transcriptome-wide polymorphisms in red abalone (*Haliotis rufescens*) from the west coast of the United States indicated signatures of local genetic adaptation correlated with carbon dioxide (CO_2) and oxygen concentrations, and involving genes associated with biomineralization, energy metabolism, heat-, and disease- or hypoxia-tolerance (De Wit & Palumbi 2013). These studies provide insights into standing genetic variation within Haliotid species for adaptation to more acidic and warmer environments emerging under climate change. They also indicate that adaptive genetic differences can persist in Haliotid species despite potential for panmixia, at least along broad geographic gradients. Selection processes may also operate at fine spatial scales in Haliotids given the heterogeneous nature of their benthic habitats, but this remains to be considered.

The current study builds on previous population genomic research on blacktip abalone (*H. rubra*) which showed a lack of overall genetic structure and evidence of a connected metapopulation spanning ~1400 km of the south-eastern Australian coastline (Miller *et al*. 2016). Here we use a hierarchical sampling regime guided by bathymetric LiDAR imagery and hindcasted oceanographic datasets to explore adaptive genetic differentiation in *H. rubra* across the same study area. Using a panel of genome wide single nucleotide polymorphism (SNP) markers derived from genomic sequencing, we contrast genetic variation among animals distributed across environmental gradients spanning local (10s to 100s of meters) to regional (100s of kilometers) spatial scales, using novel geospatial datasets. We hypothesize that selection processes operate on finer spatial scales than currently assumed in abalone species, considering: 1) the highly heterogeneous nature of abalone habitats (potential drivers of selection; Jalali *et al.* 2015), 2) the high levels of genetic polymorphism present in the species (potential gene variants for selection to act upon; Miller *et al.* 2016), and 3) pre-existing evidence for standing genetic variation associated environmental factors that vary on regional scales (evidence of existing adaptive genetic differentiation; De Wit & Palumbi 2013; Sandoval-Castillo *et al.* 2018). This study provides insights into the spatial scales of selection processes in abalone species, and identifies putative environmental factors contributing to genetic adaptation during recruitment, with implications for fisheries management.

Methods

Experimental design and sample collection

Using a combination of temperature observations from satellite data (sea surface temperature), modelled oceanographic data (wave energy, ocean currents), and LiDAR-derived seafloor structure (substrate type, VRM), we developed a hierarchical and spatially replicated sampling design comprising 29 reef locations representing different habitat types and spanning the entire Victorian coastline, encompassing the Western, Central and Eastern Zone abalone fisheries. The selection of reef locations was optimised to include populations from a range of habitat types varying in seasonal sea surface temperature (SST), local geology (substrate type and vector ruggedness measure), exposure to wave energy and ocean currents, and sea surface temperature (Table 2). Habitat maps and hindcasted oceanographic datasets indicate that each of these variables show significant heterogeneity at both local (10s to 100s of meters) and regional (100s of kilometres) scales (Ierodiaconou *et al.* 2011; Young *et al.* 2016). Temperature was a key environmental parameter as the Victorian coastline is characterised by a strong longitudinal thermal gradient driven by upwelling systems and converging ocean currents (Sandery & Kaempf 2007; Colton & Swearer 2012). Processed sea surface temperature (SST) datasets were sourced from the Integrated Marine Observing System (IMOS) – IMOS is a national collaborative research infrastructure, supported by the Australian Government. Mean winter and summer SST, and annual temperature range for the years 1995-2015 were evaluated, after which mean winter SST was omitted due to a high correlation with summer estimates. Wave energy and ocean current information were derived from a coupled hydrodynamic and wave model developed by Water Technology (more detailed information on the development of these hydrodynamic models can be found in the supplementary material). As the 500 m resolution of the hydrodynamic model did not resolve areas that were sheltered due to fine-scale coastal geometry (such as headlands and exposed offshore reefs), we calculated fetch distances in 1 degree increments from each site in a 30 degree sector, 15 degrees either side of annual mean swell direction using a custom 1:10000 scale digital coastline. Mean fetch values for each site were used to weight local estimates of wave power and orbital velocity to account for local variability in swell protection. The geology of benthic reef habitats is variable within and across regions of the Victorian coastline, and consists of basalt, calcareous and granite reef complexes. Information on substrate type for each location was inferred from existing terrestrial geology maps and inferences from bathymetric LiDAR intensity data and expert knowledge. Structure of these geologic classes was derived from the 5 m resolution LiDAR bathymetry dataset using the vector ruggedness (VRM) tool (Walbridge et al. 2018) within ArcGIS 10.5. VRM is a measure of surface roughness that is calculated using a 3 x 3 moving window where each cell in the window is assigned a VRM value based on three-dimensional location of the cell

centre, slope, and aspect (Wallbridge et al. 2018). Correlation analyses implemented in the ggpubr R package (https://cran.r-project.org/web/packages/ggpubr/index.html) confirmed the independence of all environmental variables except summer sea surface temperature and seasonal temperature range which correlated moderately (Pearson's $r = 0.6$, $P < 0.01$).

Field sampling was conducted in 2016 with the assistance of commercial survey divers contracted by the Victorian Fisheries Authority. A total of 870 abalone tissue biopsies were collected from 29 localities (30 samples per location) spanning the Victorian Western, Central and Eastern Zone fisheries and provided for genomic analysis (Table 1 and Figure 2). At each location, individual abalone were collected within a 25 m radius of an anchored vessel and were assumed a random sample of the site. Multiple size classes were intentionally sampled to avoid sampling single cohorts (potentially related individuals) that might drive ambiguous estimates of genetic structure. From these samples, we collected 50 mg tissue biopsies from each individual using sterile dissection tools to avoid cross-contamination. The biopsied material was transferred to 2-mL microcentrifuge tubes containing either 100% ethanol or RNAlater (QIAGEN) and transported to the laboratory. A total of 25 samples per location were used for genomic analysis.

DNA extraction and Genotyping by Sequencing library construction

Total genomic DNA was extracted from 10 mg of muscle tissue using the Qiagen DNeasy 96 Blood and Tissue Kit (Venlo, Limburg, NL), and reduced representation genome libraries were prepared with a modified genotyping by sequencing (GBS) protocol of Elshire *et al.* (2011). Three hundred nanograms of genomic DNA from each individual were digested in 20 µL reaction containing four units of restriction enzymes MseI and SbfI for 2 h at 37 °C. Digestion products were then ligated to modified P1 and P2 adapters with unique barcode combinations to allow for subsequent multiplexing of all individuals. Fifty µL ligations were performed containing the enzyme digested DNA, 1.125 ng of P1 and P2 adapters, 400 units of T4 ligase and T4 buffer (New England Biolabs, Beverly MA, USA). Ligations were incubated at 16 °C for 90 min followed by a 30 min of denaturation at 80 °C. Adapter ligated DNA fragments were purified using a Qiagen MinElute PCR purification kit (Redwood City, CA, USA), eluted in 20 µL of ddH20 and subsequently used for PCR amplification. Fifty µL PCRs were performed using 29 MyTaqTM HS Mix (Bioline, Taunton, MA, USA), and containing 0.2 µL each of Illumina Dual Index Sequencing Primers 1 & 2 (Illumina Inc., San Diego, CA, USA) and 10 µL of above purified DNA. PCR conditions were as follows: 95 °C for 1 min, 24 cycles of 95 °C for 30 s, 65 °C for 30 s, 72 °C for 30 s and a final extension step of 72 °C for 5 min. DNA quantitation and qualitative analysis of individual PCR products were performed on a MCE_-202 MultiNA with a DNA-1000 kit (Shimadzu, Kyoto). Samples were then pooled equimolar into groups of 71 samples (11 pooled libraries in total), with each pooled library

being sequenced on a single Illumina HiSeq 4000 (Illumina, San Diego) lane by Macrogen (Seoul, Korea).

Bioinformatics processing and genotyping

Illumina HiSeq 4000 runs yielded an average of 380 million assigned 100 base pair (bp) paired-end reads per lane, providing an average of 5.2 million paired-end reads per sample for genomic analysis. Raw sequences were first processed using the Trimmomatic V0.36 program (Bolger *et al.* 2014) by trimming the raw reads to 80 bp length and discarding all reads that had a Phred score below 20. We used the *de novo* program from *Stacks* 1.44 (Catchen *et al.* 2013) to create a catalogue of SNPs and genotypes for all individuals. Because we expected a high level of intra-population genetic diversity based on microsatellite and SNP data from a previous study (Miller *et al.* 2016), we tested several combinations of parameters that allowed *de novo* assembly of GBS loci from orthologous sequences while rejecting paralogous sequences. The final parameter settings included the maximum distance allowed between stacks (M = 3), and the distance between loci in the catalogue (n = 3), while the minimum depth of coverage to form a stack was kept constant (m = 3). SNPs and genotypes at each locus were called using a maximum likelihood framework with default *Stacks* 1.44 parameters at the significance level of 5%. A subset of polymorphic GBS loci present in at least 70% of individuals at each sampling location (Boehm *et al.* 2015; Dierickx *et al.* 2015) and having SNPs with a global minor allele frequency of $\geq$0.05 were used for downstream genomic analyses.

Estimating overall genetic structure

SNP frequencies over all loci were initially contrasted between all 29 sampled locations to determine patterns of overall genetic structure and population connectivity. Analyses were repeated following the removal of candidate loci potentially under directional selection (refer to section immediately below), but had little effect. The software GenoDive (Meirmans & Van Tienderen 2004) was used to calculate the average number of allele per locus (Na), observed (H_O) and expected (H_E) heterozygosity across loci, for each sample location, as well as global and pairwise measures of population differentiation including both F_{ST} and D_{EST} (Weir & Cockerham 1984; Jost 2008). Correlations between genetic and geographic distances were assessed using Mantel tests implemented in the adegenet package for R (Jombart 2008; Jombart & Ahmed 2011), with significance determined by permutation (10,000 randomizations). A discriminant analysis of principal components (DAPC) was implemented in the adegenet package for R (Jombart 2008; Jombart & Ahmed 2011), to obtain a graphical depiction of patterns of genetic structure. The number of genetic clusters was then defined using k-means, a clustering algorithm that looks for the value of K that maximizes the variation between groups. The Bayesian Information Criterion (BIC)

was calculated for K = 1–29 and the K value with the lowest BIC was selected as the optimal number of clusters. A discriminant analysis was then performed using the function DAPC, implemented in R, to describe the genetic clusters.

Detection of candidate SNPs

To detect putative genomic signatures of selection, we conducted genotype by environment association analyses (GEAs) using three complementary models; Latent Factor Mixed Models (LFMM; (Frichot *et al.* 2013)), the Bayesian method available in BayPass V1.01 (Gautier 2015) and redundancy analysis (RDA) (Forester *et al.* 2018). LFMM and BayPass accounted for potentially confounding allele frequency differences due to population structure in a mixed linear model framework, but in different ways: LFMM estimates GEAs when simultaneously correcting for population structure with latent factors, while BayPass uses a neutral covariance matrix constructed from population allele frequencies.

We first used LFMMs (LEA 1.3; (Frichot *et al.* 2013)) to detect genotype–environment correlations with the continuous variables described above. The number of latent factors was set to two ancestral clusters based on the cross-entropy score results using the *snmf* function in the LEA package. Cross-entropy scores evaluate the fit of the statistical model to the data using a cross-validation technique (Frichot & Francois 2015). The lowest value returned from the cross-entropy scores represents the optimal k-value and was used to correct for confounding effects from population structure in LFMM. LFMM naively imputes missing data, therefore we imputed missing data from the *snmf* run with the lowest cross-entropy score with two ancestral clusters, as described in the LFMM manual. The *lfmm* function was used in the LEA package to identify SNP-environment associations with the settings set to 10,000 iterations of the Gibbs Sampling algorithm with 5,000 burn-in iterations, outputs were averaged over 10 independent runs. The p-values were re-adjusted in *R* using the Benjamini-Hochberg method for multiple tests on the combined z-scores from all runs, as recommended in the LFMM manual (Frichot *et al.* 2013). Significance was assessed with a false discovery rate (FDR) threshold of 0.001 (i.e. q-value in LFMM terminology), as advised for these kinds of analyses (De Villemereuil *et al.* 2014).

Second, we explored GEAs with BayPass V1.01 (Gautier 2015) under the auxiliary (AUX) covariate mode (-covmcmc and -auxmode flags), after scaling the variables with the -scalecov flag. The underlying models explicitly account for the covariance structure among the population allele frequencies that originates from the shared history of the populations under study, through the estimation of the population covariance matrix Ω, which renders the identification of SNPs subjected to selection less sensitive to the confounding effect of demography (Bonhomme *et al.* 2010; Gunther & Coop 2013). The auxiliary covariate model specifically involves the introduction of a binary auxiliary variable to classify each locus as associated or not. This allows the

computation of posterior inclusion probabilities (and Bayes Factors) for each locus while explicitly accounting for multiple testing issues. For each SNP, the Bayes factor was expressed in deciban units (dB) via the transformation 10 log10 (BF). Significance was assessed based on the Bayes Factor (BF) between models and according to Jeffrey's rule (Jeffrey 1961); that is, markers with moderately ($3 < BF < 10$), strong ($10 < BF < 20$) to decisive ($BF > 20$) evidence were retained as potential candidates under positive selection.

Finally, we used redundancy analysis (RDA) to identify candidate SNPs under selection, a multivariate approach known to reduce false positive and identify unique sets of adaptive loci under weak selection (Forester *et al.* 2018). We modified R script from Forester *et al.* (2018) to test for correlations between allele frequencies and the environment by using the function *rda* implemented in the package vegan, version 2.3-5 package (Oksanen *et al.* 2013). Components of the RDA significantly correlated to the constrained axis ($a = 0.05$) were retained and a Fisher transformation was applied to correct for sample size (Bourret *et al.* 2014). SNPs were retained and considered candidates only if correlated with the retained components. In order to compare the outputs from the three methods, Venn diagrams were generated using the VennDiagram package for R (Chen & Boutros 2011).

Discriminant analysis of principal components (DAPC) were implemented in the adegenet package for R (Jombart 2008; Jombart & Ahmed 2011) to obtain a graphical depiction of patterns of genetic structure based on datasets consisting of candidate SNPs for each environmental variable identified by BayPass ($BFs > 3$), LFMM (q -values < 0.001), and RDA. As outlined previously, the number of genetic clusters was defined using k-means, with Bayesian Information Criterion (BIC) calculated for $K = 1–29$ and the K value with the lowest BIC selected as the optimal number of clusters. A discriminant analysis was then performed using the function DAPC to efficiently describe the genetic clusters.

Generalized Dissimilarity Modeling (GDM; (Ferrier *et al.* 2007)) was subsequently performed on all SNPs found to be significantly correlated with the environmental variables (derived from LFMM, BayPass and RDA analyses) following the methods described in Fitzpatrick & Keller (2015). First, F_{ST} matrices were created separately for each of the putatively adaptive SNPs using the web version of GenePop (Raymond & Rousset 1995). A GDM analysis, using the gdm package v 1.3.7 in R (Manion *et al.* 2018) was independently performed on the F_{ST} matrix for each candidate SNP to estimate allelic turnover through climatic space (deviations in allele frequency associated with environment type). GDM analysis removes variation that is associated with geographic distance and the remaining genetic variation is compared to climate (the y-axis on the spline plots generated by GDM are therefore labeled partial genetic distance). SNPs explaining zero deviance or with missing data from at least five populations were not plotted. Spline plots showed the relative importance of climate on allelic turnover, and assist in identifying

environmental thresholds where selection pressure is expected to be greatest. The significance of climate variables on the dependent variable (in this case a SNP) is calculated by the difference between two models, with and without the climate variable, and is termed deviance (Ferrier et al. 2007), which is analogous to percentage of variation explained. Note that GDM analyses could only be performed on SNPs associated with continuous environmental variables. Allelic turnover was visualised in geographic space for environmental variables SST and VRM by using pairwise F_{ST} matrices generated from the combination of SNPs deemed to be significant with its respective environmental factor based on initial GDM analyses. GDM analyses were performed on each matrix with outputs being transformed with the respective environmental raster layer using the function *gdm.transform*. Analysis of principal components was then performed on the transformed data using *prcomp*, and subsequently predicted across geographic space using the predict function (raster package) to create a raster layer comprising of allelic turnover. The results were saved as a geotiff file and visualised in ArcGIS (ESRI 2018). Analyses could not be performed for waver power or orbital velocity environmental variables as fetch corrected exposure estimates are not available for near-shore habitats at a statewide scale.

Functional annotation

Functional annotations were performed for SNP loci showing strong and significant correlations with each environmental covariable based on LFMM and BayPass (BFs > 10 and q -values < 0.00001). Tag sequences containing candidate SNP loci of interest were searched against five *Haliotis* transcriptomes: *H. laevigata* (Shiel *et al.* 2015), *H. midae* (Van Der Merwe *et al.* 2011), *H. rubra* (Deakin University, unpublished), *H. rufescens* (De Wit & Palumbi 2013), and *H. tuberculata* (Harney *et al.* 2016) using BLAST+ v2.6.0 (*blastn*, e-value 1e-5) (Camacho *et al.* 2009). Sequences with hits to any transcriptome were further annotated against the UniProtKB/Swiss-Prot protein database (Bateman *et al.* 2017) based on sequence homology (*blastx*, e-value 1e-5). Additional gene ontology term analysis was performed through InterProScan v5.28.67 (Jones *et al.* 2014) and visualized with WEGO (Ye *et al.* 2006).

Results

Genotyping and overall population structure

Genome scans of 725 *Haliotis rubra* specimens from 29 locations distributed across the Victorian western, central and eastern zone abalone fisheries were performed by reduced genome representation sequencing. Illumina sequencing yielded a total of 3,794,534,348 base paired reads, providing an average of 5.2 million base-paired reads per sample (range = 0.5 to 20.2 million). *De*

novo assembly using the STACKS bioinformatics pipeline yielded a total of 4,665,377 polymorphic GBS tags, and 1,108,067 tags containing 5,239 SNPs. Levels of diversity were largely consistent across sites with the percentage of polymorphic loci ranging from 72.7% to 96.8% (mean %P = 86.0%) (Table S1) and expected heterozygosities ranging from 0.24 to 0.28 (mean $H_E = 0.27$).

Global F_{ST} was weak but significantly different from zero ($F_{ST} = 0.009$, 95% CIs = 0.008 – 0.009; $P < 0.001$; $D_{EST} = 0.003$, 95% CIs = 0.003 – 0.004, $P < 0.001$) indicating some genetic structuring among sample locations. Significant genetic structuring appears to be associated with the Victorian eastern zone and Port Phillip Bay fishing stocks, as all pairwise F_{ST} comparisons with sites from these regions were significantly different from zero (Table S2). In contrast all pairwise estimates of F_{ST} between western zone and central zone fishing stocks (except for Port Phillip Bay) did not differ significantly from zero. Excluding the eastern zone and Port Phillip Bay fishing stocks, global F_{ST} did not differ significantly from zero ($F_{ST} = 0.002$, 95% CIs = 0 – 0.002; $P > 0.050$; $D_{EST} = 0.001$, 95% CIs = 0 – 0.001, $P > 0.050$) indicating a lack of genetic structuring between western and central zone fishing stocks. These patterns of population genetic differentiation are graphically depicted by DAPC analyses which retained 300 principal components, and the first two discriminant functions, capturing 75% of the total variance within the SNP dataset (Figure S4A), and with k-means identifying three population clusters. When plotted across the x- and y-axes, individuals from the eastern zone and Port Phillip Bay sample locations cluster separately from each other and from the main population cluster consisting of admixed individuals from the western and central zone fisheries. After removing the eastern zone and Port Phillip Bay sample locations (retaining 250 principal components, and the first two discriminant functions capturing 65% of the total variance), no genetic structuring between the western and central zone fisheries is apparent. (Figure S4B). Mantel tests showed a moderately strong relationship between genetic and geographic distance (Mantel $r = 0.43$, $P < 0.01$). This relationship is no longer significant once the sites from Port Phillip Bay and the Eastern Zone are removed from the analysis (Mantel $r = 0.01$, $P > 0.05$) consistent with high levels of gene flow across the Western and Central Zone fisheries (Figures S5A and B).

Detection of candidate SNPs

BayPass, LFMM and RDA each identified a number of candidate SNP loci exhibiting significant genotype-by-environment associations for each of the environmental covariables tested (Table 3). BayPass identified between 14 (0.26%) and 76 (1.45%) SNPs with significant correlations (log10(BF) > 3) for each of the environmental covariables (average = 49.28 SNPs; 0.94%), while a larger number of SNP loci showed significant correlations with summer SST (658 SNPs; 12.60%). LFMM identified between 12 (0.2%) and 60 SNPs (2.8%) showing significant correlations ($q < 0.001$) with each of the environmental covariables (average = 28.42 SNPs; 0.65%). Note that

because LFMM analyses could not be performed on categorical data, estimates for reef geology are not provided. RDA identified between 0 (0%) and 64 SNPs (1.2%) showing significant correlations with each of the environmental covariables, except for seasonal temperature range (average = 28.43 SNPs; 0.54%; Figure 2). For each of the environmental covariables, between 0 and 22 SNPs were identified as exhibiting significant correlations by both BayPass, LFMM and /or redundancy analyses. Venn diagrams displaying the number of candidates identified by each GEA method, and overlaps between methods, are provided in Figures S6 – 9. Overlap of candidate loci between methods was low which was expected for several reasons. Specifically, we chose GEA methods that identify candidate loci with varying sensitivities to detecting loci under weak or strong selection, use different methods for controlling for overall population structure, and adopt different yet complementary mathematical algorithms for identifying genotype-environment associations. Candidates from each GEA method were used in post-hoc analyses to better identify true positives, particularly ones that occur in genic regions (annotation) and have strong relationships with environments that cannot be explained by geography (GDM).

Discriminant Analysis of Principle Components (DAPC) was performed on SNP loci showing significant correlations with each environmental covariable based on LFMM, BayPass and RDA analyses to provide a graphical depiction of genetic structuring among environmental categories. On each occasion genetic structure was captured by the first two principal components indicated by eigenvalues in Figures 2-5, with each analysis identifying a single genetic cluster using k-means. Patterns of genetic differentiation for these loci are graphically depicted following the retention of principal components and discriminant functions that captured between 60 and 85% of the total variance. To visualise patterns of genetic structuring, populations were colour coded based on their respective habitat classifications (Figures 3 – 6). For geology, which is a categorical variable, this involved colour coding populations sampled from the various substrate types (blue = basalt, black = calcareous, red = granite; Figure 3A). For the continuous environmental variables, populations were colour coded based on relative environmental scores (low, intermediate, high; Table 2). When plotted across the x- and y-axes, patterns of genetic structuring can be seen differentiating populations from basalt, calcareous and granite reef systems. Likewise, there is genetic structuring between populations from reef complexes of low, intermediate and high VRM values (Figure 3B). For summer wave power and orbital velocity, populations with low, intermediate and high environmental values separate across the axes, but patterns associated with winter are less clear (Figures 4 and 5). DAPC plots indicate genetic structuring between populations of varying seasonal temperature ranges, while patterns associated with summer SST are not clear despite the large number of SNP loci having significant correlations with this covariate (Figure 6).

All SNPs identified as having significant associations with environmental variables were used for GDM analysis to quantify allelic turnover through climatic space (Figure 7; Table 4). The three environmental variables that explained the greatest deviance on average were winter wave power (5.31%), VRM (6.42%), and summer wave power (9.55%). In contrast, seasonal temperature range explained the least deviance, with only one SNP explaining a very low (0.28%) level of variation, as presented in the spline plot in Table 4. The majority of SNPs plotted against each environmental variable showed small to moderate responses to climate (i.e. deviance explained; Table 4). However, several SNPs explained greater than 10% of the variation, suggesting directional selection. For example, winter wave power associated with SNPs 94891_79 and 29000_33 and showed strong clines with deviances of 13.47% and 13.2%, respectively; summer wave power associated with SNPs 12085_77, 14150_22, and 29000_33 and had deviances of 17.68%, 24.21%, and 14.88%, respectively; summer sea surface temperature associated with SNP 15442_53 had a deviance of 22.03%; and VRM associated SNPs 15487_52 and 35093_14 and showed strong clines with deviances of 18.96% and 18.12% (Table 4). In contrast, SNPs associated with summer and winter orbital velocity explained little variation (< 5% deviance). The GDM spline plots also demonstrate defined points of allelic turn-over for many SNPs in climate space (Figure 7). Specifically, allelic turn-over occurs at five and three kW/m for winter and summer wave power (Figure 7A and B), approximately 18 ^{O}C for summer sea surface temperature (Figure 7C), and 0.0009 for VRM (Figure 7G). These values may be interpreted as environmental thresholds influencing selection and separating adaptive genotypes but should be treated with caution due to the shallow genome coverage dataset used in this study. These thresholds are further depicted by allelic turnover maps which show two very distinct patterns of selection: broad-scale turnover in SST where allelic changes occur at regional scales (Figure 8A) and fine-scale turnover in VRM where allelic changes occur at local spatial scales (Figure 8B).

Functional Annotation

Tag sequences containing candidate SNP loci which showed strong and significant correlations with each environmental covariable were searched against five *Haliotis* transcriptomes. An average of 36% of tags (range 25 – 57%) were confidently aligned to *Haliotis* transcripts, with an average of 16% (range 5 – 27%) having annotations for genes associated with molecular function, biological processes and cellular components. All functional annotations are provided in Table S3.

Discussion

Evidence of adaptive genetic structuring despite gene flow

Using a sampling regime informed by high-resolution bathymetric and hindcasted oceanographic datasets, we contrasted patterns of genetic variation in *H. rubra* across heterogeneous habitats and

~1,400 km of Australia's south eastern coastline. Estimates of overall genetic structure are consistent with previous studies (Brown 1991; Conod *et al.* 2002; Li *et al.* 2006; Miller *et al.* 2016), indicating a lack of genetic differentiation and potential panmixia across almost 1,000 km's of the sampling range, extending from the South Australian border to Wilsons Promontory located on the east-central coast of Victoria. Populations from the eastern extreme of the sampling range (east of Wilson Promontory) and Port Phillip Bay appear weakly differentiated, as demonstrated by previous studies (Brown 1991; Conod *et al.* 2002; Miller *et al.* 2016). Biogeographic structuring of marine communities and limitations to gene flow among populations separated by Wilson Promontory is well-recognised (York *et al.* 2008; Ayre *et al.* 2009; Colton & Swearer 2012; Miller *et al.* 2013), and has been attributed to historical (Lambeck & Chappell 2001) and contemporary physical oceanographic factors, such as converging ocean currents, environmental gradients (temperature and salinity) and habitat discontinuities that persist in the region (Baines *et al.* 1983; Ridgway & Godfrey 1997; Ridgway & Condie 2004; Sandery & Kaempf 2007; Colton & Swearer 2012). Weak differentiation of Port Phillip Bay is also consistent with the oceanography of the region, with the low flushing rates of Port Phillip Bay (~270 days; (Walker 1999) expected to limit gene flow between local populations and those from outside coastal waters. Despite a lack of genetic structure across much of the Victorian coastline, we provide evidence for genotype associations with heterogeneous habitat features occurring at local and regional spatial scales which are likely driving patterns of adaptive genetic structuring within *H. rubra*.

Drift processes leading to neutral genetic structure are often suppressed in broadcast spawning marine organisms with large populations sizes (Waples 1998; Whitlock & Mccauley 1999; Hauser & Carvalho 2008), but numerous studies have shown that adaptive genetic divergences can still be established and maintained under strong selection pressure (Marshall *et al.* 2010; Milano *et al.* 2014; Torda *et al.* 2017). This appears applicable to *Haliotis* species where studies on Western Australian greenlip and Californian red abalone indicate selection contributing to genetic adaptations associated with broad regional temperature, oxygen, and acidity gradients, despite a lack of overall genetic structure (De Wit & Palumbi 2013; Sandoval-Castillo *et al.* 2015; Sandoval-Castillo *et al.* 2018). We provide additional support, with evidence of adaptive divergence associated with a temperature gradient in *H. rubra*. We are cautious with the interpretation of these findings due to the high number of SNP loci found to be associated with sea surface temperature (~10% of total SNPs). The possible influence of artefactual associations (i.e. false positives) and SNP associations with other environmental factors varying with longitude cannot be ruled out. It is also possible that adaptive loci are contained within inversions, which create genomic areas of linkage disequilibrium (Hoffmann & Rieseberg, 2008) and have been implicated in many recent examples of adaptive divergence (Twyford & Friedman 2015; Kirubakaran *et al.* 2016). Yet, the previous reports of temperature as a driver of local adaptation in other Haliotid species suggests our

results may at least partly reflect temperature-related genetic structuring which warrants further investigation.

Our data also point to the possibility of selection associated with heterogeneous habitat features occurring on more local spatial scales. Specifically, our genotype-environmental association analyses suggest genotype associations with habitat features such as local reef geology, reef complexity, and exposure to wave power and ocean currents that vary over scales of 10s to 100s of meters (Ierodiaconou *et al.* 2011; Young *et al.* 2016). Evidence of fine scale adaptive genetic structuring is unusual in dispersive marine species, with a few exceptions (Sherman *et al.* 2008; Babin *et al.* 2017). While we cannot completely rule out the influence of false positives, each genotype–environment association (GEA) detected was corrected for spatial structure and distance, and our sampling regime contrasted genetic variation across distinct habitat types present both within and between western, central, and eastern regions of the state. Also, the largely panmictic nature of the *H. rubra* population spanning our sampling area suggests that artefactual demographic factors capable of producing 'selection-like' signatures across the genome (i.e. such as allelic surfing (Excoffier & Ray 2008)), are unlikely to influence our results.

At this stage it is uncertain if habitat features are directly or indirectly influencing genotype distributions. For example, substrate type (i.e. basalt, calcareous, granite) can influence benthic community composition, biological interactions and resource availability (Edmunds *et al.* 2000) . Likewise, VRM is a physical measure of seabed complexity which can also influence benthic community compositions and biological interactions, as well as wave energy exposure, local oxygen saturation levels, and nutrient and resource availability (Sappington *et al.* 2007; Young *et al.* 2010; Martin-Garcia *et al.* 2013). This is also true for subtidal reefs that vary with respect to exposure to wave power and ocean currents (Young *et al.* 2015). As a result, the exact drivers of selection and potential adaptive divergence in *H. rubra* are unclear and warrant further investigation. Interestingly, our results suggest that variation in summer wave power and orbital velocity may lead to stronger patterns of local adaptation compared with winter months. This may reflect the *H. rubra* life cycle, where spawning typically occurs during the warmer months of the year (between February and April and again between October and December (Mcshane & Smith 1991)) when selection is likely to be strongest, acting on early life stages (Fraser *et al.* 2008; Postma & Ågren 2016). Experimental manipulations (i.e. via thermal stress, transplant, and common garden experiments) coupled with genome resequencing will assist in identifying environmental factors directly influencing selection and the genes and genomic features underpinning local adaptations (Jones *et al.* 2012; Berg *et al.* 2017; Price *et al.* 2018).

Insights into environmental resilience and recruitment processes

570 Results from this study are relevant to the potential resilience of *H. rubra* populations to
571 continued exploitation and changing environmental conditions. Marine ecosystems around the
572 world are experiencing rapid environmental transformations with climate change contributing to
573 rising ocean temperatures, the build-up of anthropogenic CO_2, changing ocean currents, and major
574 shifts in seasonal weather patterns (Hoegh-Guldberg & Bruno 2010; Burrows *et al.* 2011; Wernberg
575 *et al.* 2011). This is particularly pertinent in south-eastern Australia where ocean temperatures are
576 warming at four times the global average and ocean currents are strengthening and extending
577 southward (Ridgway 2007). Our results suggest potential genetic adaptations to temperature, wave
578 energy and current intensity, as well as connectivity between locations that show geographical
579 variation in them. This suggests standing genetic variation may be available for selection to act on
580 to counter future environmental change, assisted by wide spread gene flow and a short generation
581 time in this species (~4 years; (Andrews 1999)). This is a timely finding given abalone populations
582 around the world are showing signs of climate change stress, with depletion events in recent years
583 associated with exposure to extreme temperatures (Pearce *et al.* 2011; Micheli *et al.* 2012; Boch *et*
584 *al.* 2018). Quantitative tests via thermal stress, transplant, and common garden experiments, will
585 help to validate our findings, and provide information on the potential role of plasticity and genetic
586 adaptation in assisting *Haliotis* species counter climate change.
587 Abiotic factors such as local current intensities and wave energy are expected to determine
588 distances and directionalities of larvae movement (Treml *et al.* 2015). However, selection is
589 potentially playing a role in determining habitats to which larvae can recruit depending on their
590 adaptive or maladaptive genetic background. For example, larvae released into the water column
591 from low energy environments are expected to be maladapted to high energy environments, and
592 may not successfully recruit to high energy habitat patches despite dispersal potential. This is not a
593 novel finding; evidence of phenotype-environment mismatches impacting recruitment dynamics
594 and reducing population connectivity in dispersive marine species is well documented and
595 summarised in Marshall *et al.* (2010). Natural selection could potentially occur at pre- or post-
596 settlement stages in *H. rubra,* as seen in other marine and diadromous taxa (Sherman *et al.* 2008;
597 Babin *et al.* 2017). In some marine species, environmental cues influence the settlement of larvae
598 from the water column (Rodriguez *et al.* 1993; Harrington *et al.* 2004; Sneed *et al.* 2014), with
599 encrusting coralline algae, macroalgae, and mucus trails reported to be potential settlement cues for
600 Haliotids (Morse *et al.* 1984; Takami *et al.* 1997; Huggett *et al.* 2005). Consequently, it is possible
601 that abalone larvae with different genotypes respond to specific cues, maximising the chance of
602 successful recruitment by settling upon suitable habitats, as shown in some corals (Meyer *et al.*
603 2009). Conversely, selection may act post-settlement, where maladapted genotypes are selected
604 against. For example, genetic inviability driven by genotype-environment interactions may be
605 responsible for high juvenile mortality in oysters (Plough 2012; Plough *et al.* 2016). As post-

606 settlement juvenile mortality is extremely high in *Haliotis* species (Mcshane & Smith 1991;
607 Kiyomoto 2007), post-settlement selection warrants further investigation. Overall, these findings
608 suggest that recruitment processes in Haliotids are likely to be complicated, with a combination of
609 exogenous and endogenous factors, including selection processes, having an influence.
610
611 *Further implications for fisheries management*
612 Translocation and reseeding activities are common management tools used for establishing new
613 fishing stocks and to catalyse the recovery of depleted stocks, including abalone fisheries (Bell *et*
614 *al.* 2005; Roberts *et al.* 2007; Taniguchi *et al.* 2013). In recent years translocations have been
615 undertaken across *H. rubra* fisheries to assist the recovery of virus and urchin affected stocks in
616 south-eastern Australia (Department of Primary Industries 2012). Our results suggest that managers
617 should pay careful attention to the selection of genetically suitable animals for translocation
618 purposes, either through prior genotyping or habitat matching, to maximise return on investment.
619 The environmental thresholds driving allelic turn-over in our GDM spline plots could be used for
620 such purposes. Failure to consider the genetic profiles of fishing stocks could lead to the movement
621 of animals that are maladapted to their new habitat and lead to stocking failure. Indeed, the failure
622 of many restoration programs within the native ranges of Pacific salmon has been suggested to
623 partly result from inadequate adaptive 'matching' of translocated populations to their new
624 environments (Allendorf & Waples 1996).
625
626
627
628
629 **Conclusion**
630 Population genomic studies offer the opportunity to characterise selection processes and
631 environmental factors that contribute to genetic adaptation at species and population levels. Such
632 studies can assist management by providing insights into the likely resilience of species to
633 environmental change, and the influences of migration and selection on recruitment processes. The
634 current study demonstrates how emerging geospatial datasets offer new opportunities for
635 quantifying patterns of habitat heterogeneity in marine systems, and contrasting genetic variation
636 across environmental gradients to identify signatures and environmental drivers of selection with
637 unprecedented sensitivity. This research is becoming increasingly important as marine ecosystems
638 around the world are facing increasing threats from climate change, invasive pests, disease and
639 resource exploitation. Effective marine conservation planning and fisheries management, based on
640 population genomic studies with geospatially informed sampling regimes, will assist in minimizing
641 biodiversity loss and sustainable exploitation of commercially targeted species into the future.

Acknowledgements

This project was funded by the Fisheries Research and Development Corporation (FRDC) project '2015-025: Patterns of interaction between habitat and oceanographic variables affecting the connectivity and productivity of invertebrate fisheries' on behalf of the Australian Government, plus contributions from the Western Abalone Divers Association. We thank Nick Murphy (La Trobe University), Steve Swearer (The University of Melbourne), and Jan Strugnell (James Cook University) for their contributions to the original project proposal. We would also like to thank Harry Gorfine from the Victorian Fisheries Authority, and government contract divers David Forbes and Johno Rudge and their respective crews, for their assistance with the genetic sampling. Additional thanks to Chris Austin, Han Ming Gan and Yin Peng Lee (Deakin University), for assistance with generation of genomics libraries and sequencing.

This project was conceived by A.D.M and C.D.H, and experimental design was assisted by AAH. A.D.M, C.D.H., M.H.T., and M.C., were responsible for generating the data, and the analysis was led by A.D.M with assistance from M.H.T., C.A., C.D.H., and A.A.H. Geospatial datasets were provided by M.Y., A.R., D.A.I., and E.T. Writing of the manuscript was led by A.D.M. with assistance from all authors.

Data accessibility

Genomic and environmental data sets, and scripts for GEA analyses are available in the DRYAD archives under accession doi:10.5061/dryad.kb401ch

Table 1 Sites included in genomic analysis

Table 2 Summary of environmental statistics for all 29 collection sites: geology, Vector Ruggedness Measure (VRM), average winter and summer wave power (kW/m); average winter and summer orbital velocity (m/s); average summer and seasonal range in sea surface temperature (^{O}C)

Table 3 Numbers of candidate loci identified as having significant correlations with environmental covariables by BayPass and Latent Factor Mixed Models (LFMM) from a total dataset of 5,239 SNPs.

Figure 1 Sampling locations for population genomic analysis from south-eastern Australia, including the western (inset figure 'a'), central (inset figures 'b, c, d and e'), and eastern (inset figure 'f') zone fisheries. Refer to Table 1 for sample codes. Wilsons Promontory visible within inset 'e'.

Figure 2 Identification of SNPs under putative selection using redundancy analysis. All points are SNPs, off-white points are SNPs not associated with the 8 environmental variables. Colours signify significant correlation with environmental variables. The "GRA" inertia is not shown in the RDA plot because it was used as the 'dummy' variable for the remaining two geological states ("BAS" and "CAL"). SWP = summer wave power; VRM = vector ruggedness measure; WWP = winter wave power; WOV = winter orbital velocity; SOV = summer orbital velocity; SST = summer seasonal temperature; STR = seasonal range sea surface temperature; BAS = geology (basalt); CAL = geology (calcareous); GRA = geology (granite).

Figure 3 Discriminant analysis of principal components plots based on candidate SNPs putatively under selection and associated with habitat geology (substrate and VRM). Inset eigenvalues indicate the number of two principal components that captured the observed genetic structure**.**

Figure 4 Discriminant analysis of principal components plots based on candidate SNPs associated with winter and summer wave power. Inset eigenvalues indicate the number of two principal components that captured the observed genetic structure.

Figure 5 Discriminant analysis of principal components plots based on candidate SNPs associated with winter and summer orbital velocity. Inset eigenvalues indicate the number of two principal components that captured the observed genetic structure.

Figure 6 Discriminant analysis of principal components plots based on candidate SNPs associated with summer sea surface temperature and seasonal temperature range. Inset eigenvalues indicate the number of two principal components that captured the observed genetic structure.

Figure 7 Generalized Dissimilarity Modeling spline plots quantifying allelic turnover through climatic space (deviations in allele frequency associated with environment type) for candidate SNPs

putatively associated with environmental variables a) winter wave power, b) summer wave power, c) summer seasonal temperature, d) seasonal range sea surface temperature, e) winter orbital velocity, f) summer orbital velocity, g) vector ruggedness measure. Individual lines represent allelic turn over for single loci.

Figure 8 Predicted spatial turnover in allele frequencies of *H. rubra* based on generalised dissimilarity modeling analyses for all SNPs associated with a) summer sea surface temperature, and b) vector ruggedness measure. Regions with similar colours are expected to harbor populations with similar genomic compositions. Sediment habitats which are uninhabited by abalone and shown in grey.

References

Ahrens CW, Rymer PD, Stow A, Bragg J, Dillon S *et al.* (2018) The search for loci under selection: trends, biases and progress. *Molecular Ecology* **27:** 1342-1356.

Allendorf FW, and Waples RS (1996) Conservation and genetics of salmonid fishes, pp. 238-280 in *Conservation Genetics: Case Histories from Nature*, edited by Avise JC and Hamrick JL. Chapman and Hall, New York.

Andrews NL (1999) *Under Southern Seas: The Ecology of Australia's Rocky Reefs*. University of New South Wales Press, Sydney.

Ayre DJ, Minchinton TE and Perrin C (2009) Does life history predict past and current connectivity for rocky intertidal invertebrates across a marine biogeographic barrier? *Molecular Ecology* **18:** 1887-1903.

Babin C, Gagnaire PA, Pavey SA, Bernatchez L (2017) RAD-Seq reveals patterns of additive polygenic variation caused by spatially-varying selection in the American Eel (*Anguilla rostrata*). *Genome Biology and Evolution* **9:** 2974–2986.

Baines PG, Edwards RJ and Fandry CB (1983) Observations of a new baroclinic current along the western continental slope of Bass Strait. *Australian Journal of Marine and Freshwater Research* **34:** 155-157.

Bateman A, Martin MJ, O'Donovan C, Magrane M, Alpi E *et al.* (2017) UniProt: the universal protein knowledgebase. *Nucleic Acids Research* **45:** D158-D169.

Bell JD, Rothlisberg PC, Munro JL, Loneragan NR, Nash WJ *et al.* (2005) Restocking and Stock Enhancement of Marine Invertebrate Fisheries. *Restocking and Stock Enhancement of Marine Invertebrate Fisheries* **49:** 1-374.

743 Berg PR, Star B, Pampoulie C, Bradbury IR, Bentzen P, Hutchings JA, Trans-oceanic genomic
744 divergence of Atlantic cod ecotypes is associated with large inversions
745 Boch CA, Micheli F, AlNajjar M, Monismith SG, Beers JM *et al.* (2018) Local oceanographic
746 variability influences the performance of juvenile abalone under climate change. *Scientific*
747 *Reports* **8:** 5501.
748 Boehm JT, Waldman J, Robinson JD and Hickerson MJ (2015) Population genomics reveals
749 seahorses (*Hippocampus erectus*) of the western mid-Atlantic coast to be residents rather
750 than vagrants. *Plos One* **10:** e0116219.
751 Bolger AM, Lohse M and Usadel B (2014) Trimmomatic: a flexible trimmer for Illumina sequence
752 data. *Bioinformatics* **30:** 2114-2120.
753 Bonhomme M, Chevalet C, Servin B, Boitard S, Abdallah J *et al.* (2010) Detecting Selection in
754 Population Trees: The Lewontin and Krakauer Test Extended. *Genetics* **186:** 241-U406.
755 Bourret V, Dionne M, & Bernatchez L (2014). Detecting genotypic changes associated with
756 selective mortality at sea in Atlantic salmon: polygenic multilocus analysis surpasses
757 genome scan. *Molecular Ecology* **23:** 4444-4457.
758 Brock JC, and Purkis SJ (2009) The Emerging Role of Lidar Remote Sensing in Coastal Research
759 and Resource Management. *Journal of Coastal Research* **25:** 1-5.
760 Brown CJ, Smith SJ, Lawton P and Anderson JT (2011) Benthic habitat mapping: A review of
761 progress towards improved understanding of the spatial ecology of the seafloor using
762 acoustic techniques. *Estuarine Coastal and Shelf Science* **92:** 502-520.
763 Brown LD (1991) Genetic variation and population structure in the blacklip abalone, *Haliotis*
764 *rubra*. *Australian Journal of Marine and Freshwater Research* **42:** 77-90.
765 Buehler D, Poncet BN, Holderegger R, Manel S, Taberlet P *et al.* (2013) An outlier locus relevant
766 in habitat-mediated selection in an alpine plant across independent regional replicates.
767 *Evolutionary Ecology* **27:** 285-300.
768 Burrows MT, Schoeman DS, Buckley LB, Moore P, Poloczanska ES *et al.* (2011) The Pace of
769 Shifting Climate in Marine and Terrestrial Ecosystems. *Science* **334:** 652-655.
770 Camacho C, Coulouris G, Avagyan V, Ma N, Papadopoulos J *et al.* (2009) BLAST plus :
771 architecture and applications. *Bmc Bioinformatics* **10**: 421.
772 Catchen J, Hohenlohe PA, Bassham S, Amores A and Cresko WA (2013) Stacks: an analysis tool
773 set for population genomics. *Molecular Ecology* **22:** 3124-3140.
774 Chambers MD, VanBlaricom GR, Hauser L, Utter F and Friedman CS (2006) Genetic structure of
775 black abalone (*Haliotis cracherodii*) populations in the California islands and central
776 California coast: Impacts of larval dispersal and decimation from withering syndrome.
777 *Journal of Experimental Marine Biology and Ecology* **331:** 173-185.

778 Chen H, Boutros PC (2011) VennDiagram: a package for the generation of highly-customizable
779 Venn and Euler diagrams in R. *BMC Bioinformatics* **12**:35
780 Cogan CB, Todd BJ, Lawton P and Noji TT (2009) The role of marine habitat mapping in
781 ecosystem-based management. *Ices Journal of Marine Science* **66:** 2033-2042.
782 Colton MA, and Swearer SE (2012) Locating faunal breaks in the nearshore fish assemblage of
783 Victoria, Australia. *Marine and Freshwater Research* **63:** 218-231.
784 Conod N, Bartlett JP, Evans BS and Elliott NG (2002) Comparison of mitochondrial and nuclear
785 DNA analyses of population structure in the blacklip abalone *Haliotis rubra* Leach. *Marine*
786 *and Freshwater Research* **53:** 711-718.
787 Davey JW, Hohenlohe PA, Etter PD, Boone JQ, Catchen JM *et al.* (2011) Genome-wide genetic
788 marker discovery and genotyping using next-generation sequencing. *Nature Reviews*
789 *Genetics* **12:** 499-510.
790 Department of Primary Industries (2012) A review of rebuilding options for the Victorian abalone
791 fishery. Fisheries Victoria Management Report, State Government of Victoria.
792 de Villemereuil P, Frichot E, Bazin E, Francois O and Gaggiotti OE (2014) Genome scan methods
793 against more complex models: when and how much should we trust them? *Molecular*
794 *Ecology* **23:** 2006-2019.
795 De Wit P, and Palumbi SR (2013) Transcriptome-wide polymorphisms of red abalone (*Haliotis*
796 *rufescens*) reveal patterns of gene flow and local adaptation. *Molecular Ecology* **22:** 2884-
797 2897.
798 Dierickx EG, Shultz AJ, Sato F, Hiraoka T and Edwards SV (2015) Morphological and genomic
799 comparisons of Hawaiian and Japanese Black-footed Albatrosses (*Phoebastria nigripes*)
800 using double digest RADseq: implications for conservation. *Evolutionary Applications* **8:**
801 662-678.
802 Edmunds M, Chidgey S and Willcox S (2000) Environmental Inventory of Victoria's Marine
803 Ecosystems Stage 3, edited by Ferns LW and Hough D. Parks, Flora and Fauna Division,
804 Department of Natural Resources and Environment, East Melbourne, Australia.
805 Ekblom R, and Galindo J (2011) Applications of next generation sequencing in molecular ecology
806 of non-model organisms. *Heredity* **107:** 1-15.
807 Elshire RJ, Glaubitz JC, Sun Q, Poland JA, Kawamoto K *et al.* (2011) A Robust, Simple
808 Genotyping-by-Sequencing (GBS) Approach for High Diversity Species. *Plos One* **6**.
809 Environmental Systems Research Institute (ESRI) 2018. ArcGIS Release 10.5. Redlands, CA.
810 Excoffier L, and Ray N (2008) Surfing during population expansions promotes genetic revolutions
811 and structuration. *Trends in Ecology & Evolution* **23:** 347-351.

812 Ferrier S, Manion G, Elith J and Richardson K (2007) Using generalized dissimilarity modelling to
813 analyse and predict patterns of beta diversity in regional biodiversity assessment. *Diversity*
814 *and Distributions* **13:** 252-264.
815 Fitzpatrick MC, and Keller SR (2015) Ecological genomics meets community-level modelling of
816 biodiversity: mapping the genomic landscape of current and future environmental
817 adaptation. *Ecology Letters* **18:** 1-16.
818 Forester, BR, Lasky JR, Wagner HH, and Urban DL (2018). Comparing methods for detecting
819 multilocus adaptation with multivariate genotype–environment associations. *Molecular*
820 *Ecology* **27:** 2215-2233.
821 Fraser DJ, Cook AM, Eddington JD, Bentzen P and Hutchings JA (2008) Mixed evidence for
822 reduced local adaptation in wild salmon resulting from interbreeding with escaped farmed
823 salmon: complexities in hybrid fitness. *Evolutionary Applications* **1:** 501-512.
824 Frichot E, and Francois O (2015) LEA: An R package for landscape and ecological association
825 studies. *Methods in Ecology and Evolution* **6:** 925-929.
826 Frichot E, Schoville SD, Bouchard G and Francois O (2013) Testing for Associations between Loci
827 and Environmental Gradients Using Latent Factor Mixed Models. *Molecular Biology and*
828 *Evolution* **30:** 1687-1699.
829 Galindo J, Martinez-Fernandez M, Suarez P, Moran P, Juan FS *et al.* (2009) The adaptive role of
830 Phosphoglucomutase and other allozymes in a marine snail across the vertical rocky-shore
831 gradient. *Biological Journal of the Linnean Society* **98:** 225-233.
832 Gautier M (2015) Genome-wide scan for adaptive divergence and association with population-
833 specific covariates. *Genetics* **201:** 1555-1579.
834 Gordon HR, and Cook PA (2013) World abalone supply, markets, and pricing: 2011 update.
835 *Journal of Shellfish Research* **32:** 5-7.
836 Gruenthal KM, Acheson LK and Burton RS (2007) Genetic structure of natural populations of
837 California red abalone (*Haliotis rufescens*) using multiple genetic markers. *Marine Biology*
838 **152:** 1237-1248.
839 Gruenthal KM, and Burton RS (2005) Genetic diversity and species identification in the endangered
840 white abalone (*Haliotis sorenseni*). *Conservation Genetics* **6:** 929-939.
841 Gruenthal KM, and Burton RS (2008) Genetic structure of natural populations of the California
842 black abalone (*Haliotis cracherodii* Leach, 1814), a candidate for endangered species status.
843 *Journal of Experimental Marine Biology and Ecology* **355:** 47-58.
844 Grummer JA, Beheregary LB, Bernatchez L, Hand BK, Luikart G, Narum S, Taylor EB (2019)
845 Aquatic landscape genomics and environmental effects on genetic variation. *Trends in*
846 *Ecology and Evolution*. DOI.org/10.1016/j.tree.2019.02.013.

847 Gunther T, and Coop G (2013) Robust identification of local adaptation from allele frequencies.
848 *Genetics* **195:** 205-220.
849 Hahn KO (1988) Larval development of abalone, pp. 71-99 in *The Culture of Abalone and Other*
850 *Marine Gastropods*, edited by Hahn KO. CRC Press, Boca Raton.
851 Harney E, Dubief B, Boudry P, Basuyaux O, Schilhabel MB *et al.* (2016) De novo assembly
852 and annotation of the European abalone *Haliotis tuberculata* transcriptome. *Marine*
853 *Genomics* **28:** 11-16.
854 Harrington L, Fabricius K, De'ath G and Negri A (2004) Recognition and selection of settlement
855 substrata determine post-settlement survival in corals. *Ecology* **85:** 3428-3437.
856 Hauser L, and Carvalho GR (2008) Paradigm shifts in marine fisheries genetics: ugly hypotheses
857 slain by beautiful facts. *Fish and Fisheries* **9:** 333-362.
858 Hemer MA, Fan YL, Mori N, Semedo A and Wang XLL (2013) Projected changes in wave climate
859 from a multi-model ensemble. *Nature Climate Change* **3:** 471-476.
860 Hess JE, Campbell NR, Close DA, Docker MF and Narum SR (2013) Population genomics of
861 Pacific lamprey: adaptive variation in a highly dispersive species. *Molecular Ecology* **22:**
862 2898-2916.
863 Hoegh-Guldberg O, and Bruno JF (2010) The Impact of Climate Change on the World's Marine
864 Ecosystems. *Science* **328:** 1523-1528.
865 Hoffmann AA, and Sgro CM (2011) Climate change and evolutionary adaptation. *Nature* **470:** 479-
866 485.
867 Hoffmann AA, and Rieseberg LH (2008) Revisiting the impact of inversions in evolution: from
868 population genetic markers to drivers of adaptive shifts and speciation? *Annual Review of*
869 *Ecology, Evolution, and Systematics* **39:** 21-42.
870 Huggett MJ, de Nys R, Williamson JE, Heasman M and Steinberg PD (2005) Settlement of larval
871 blacklip abalone, *Haliotis rubra*, in response to green and red macroalgae. *Marine Biology*
872 **147:** 1155-1163.
873 Ierodiaconou D, Monk J, Rattray A, Laurenson L and Versace VL (2011) Comparison of automated
874 classification techniques for predicting benthic biological communities using hydroacoustics
875 and video observations. *Continental Shelf Research* **31:** S28-S38.
876 Ierodiaconou DA, Young M, Miller AD, Treml E, Swearer S *et al.* (2018) Patterns of interaction
877 between habitat and oceanographic variables affecting the connectivity and productivity of
878 invertebrate fisheries. Fisheries Research and Development Corporation (Final report, 2015-
879 025).
880 Jalali MA, Ierodiaconou D, Gorfine H, Monk J and Rattray A (2015) Exploring spatiotemporal
881 trends in commercial fishing effort of an abalone fishing zone: A GIS-based hotspot model.
882 *Plos One* **10:** e0122995.

Jeffreys H (1961) Theory of Probability (3rd edition). Oxford: Oxford University Press.

Jombart T (2008) adegenet: a R package for the multivariate analysis of genetic markers. *Bioinformatics* **24:** 1403-1405.

Jombart T, and Ahmed I (2011) adegenet 1.3-1: new tools for the analysis of genome-wide SNP data. *Bioinformatics* **27:** 3070-3071.

Jones FC, Grabherr MG, Chan YF, Russell P, Mauceli E *et al.* (2012) The genomic basis of adaptive evolution in threespine sticklebacks. *Nature* **484:** 55-61.

Jones P, Binns D, Chang HY, Fraser M, Li WZ *et al.* (2014) InterProScan 5: genome-scale protein function classification. *Bioinformatics* **30:** 1236-1240.

Jordan R, Hoffmann AA, Dillon SK and Prober SM (2017) Evidence of genomic adaptation to climate in *Eucalyptus microcarpa*: Implications for adaptive potential to projected climate change. *Molecular Ecology* **26:** 6002-6020.

Jost l (2008) Gst and its relatives do not measure differentiation. *Molecular Ecology* **17:** 4015-4026.

Kashiwada JV, and Taniguchi IK (2007) Application of recent red abalone *Haliotis rufescens* surveys to management decisions outlined in the California Abalone Recovery and Management Plan. *Journal of Shellfish Research* **26:** 713-717.

Kirubakaran TG, Grove H, Kent MP, *et al*. (2016) Two adjacent inversions maintain genomic differentiation between migratory and stationary ecotypes of Atlantic cod. *Molecular Ecology* **25:** 2130-2143.

Kiyomoto S (2007) The presence of scavengers increases the vulnerability of juvenile abalone to predatory fish. *Fisheries Science* **73:** 732-734.

Kough AS, Claro R, Lindeman KC and Paris CB (2016) Decadal analysis of larval connectivity from Cuban snapper (Lutjanidae) spawning aggregations based on biophysical modeling. *Marine Ecology Progress Series* **550:** 175-190.

Lambeck K, and Chappell J (2001) Sea level change through the last glacial cycle. *Science* **292:** 679-686.

Lecours V, Lucieer VL, Donlan MFJ and Micallef A (2015) An ocean of possibilities: applications and challenges of marine geomorphometry in *Geomorphometry for geosciences*, edited by Zwolinski Z, Mitasova H and Hengl T. International Society for Geomorphometry, Poznan, Poland.

Leiva GE, and Castilla JC (2001) A review of the world marine gastropod fishery: evolution of catches, management and the Chilean experience. *Reviews in Fish Biology and Fisheries* **11:** 283-300.

Li ZB, Appleyard SA and Elliott NG (2006) Population structure of *Haliotis rubra* from South Australia inferred from nuclear and mtDNA analyses. *Acta Oceanologica Sinica* **25:** 99-112.

Manion G, Lisk M, Ferrier S, Nieto-Lugilde D and Fitzpatrick MC (2018) GDM: Functions for Generalized Dissimilarity Modeling; R Package Version 1.2.3.

Marshall DJ, Monro K, Bode M, Keough MJ and Swearer S (2010) Phenotype-environment mismatches reduce connectivity in the sea. *Ecology Letters* **13:** 128-140.

Martin-Garcia L, Gonzalez-Lorenzo G, Brito-Izquierdo IT and Barquin-Diez J (2013) Use of topographic predictors for macrobenthic community mapping in the Marine Reserve of La Palma (Canary Islands, Spain). *Ecological Modelling* **263:** 19-31.

Martinez-Fernandez M, Bernatchez L, Rolan-Alvarez E and Quesada H (2010) Insights into the role of differential gene expression on the ecological adaptation of the snail *Littorina saxatilis*. *BMC Evolutionary Biology* **10:** 356.

Mayer L, Jakobsson M, Allen G, Dorschel B, Falconer R *et al.* (2018) The Nippon Foundation-GEBCO Seabed 2030 Project: The Quest to See the World's Oceans Completely Mapped by 2030. *Geosciences* **8:** 63.

McShane PE, Black KP and Smith MG (1988) Recruitment processes in *Haliotis rubra* Leach (Mollusca: Gastropoda) and regional hydrodynamics in southeastern Australia imply localized dispersal of larvae. *Journal of Experimental Marine Biology and Ecology* **124:** 175-203.

McShane PE, and Smith MG (1991) Recruitment variation in sympatric populations of *Haliotis rubra* (Mollusca, Gastropoda) in southeast Australian waters. *Marine Ecology Progress Series* **73:** 203-210.

Meirmans PG, and Van Tienderen PH (2004) GENOTYPE and GENODIVE: two programs for the analysis of genetic diversity of asexual organisms. *Molecular Ecology Notes* **4:** 792-794.

Meyer E, Davies S, Wang S, Willis BL, Abrego D *et al.* (2009) Genetic variation in responses to a settlement cue and elevated temperature in the reef-building coral *Acropora millepora*. *Marine Ecology Progress Series* **392:** 81-92.

Micheli F, Saenz-Arroyo A, Greenley A, Vazquez L, Montes JAE *et al.* (2012) Evidence That Marine Reserves Enhance Resilience to Climatic Impacts. *Plos One* **7:** e40832.

Milano I, Babbucci M, Cariani A, Atanassova M, Bekkevold D *et al.* (2014) Outlier SNP markers reveal fine-scale genetic structuring across European hake populations (*Merluccius merluccius*). *Molecular Ecology* **23:** 118-135.

Miller AD, van Rooyen A, Rasic G, Ierodiaconou DA, Gorfine HK *et al.* (2016) Contrasting patterns of population connectivity between regions in a commercially important mollusc *Haliotis rubra*: integrating population genetics, genomics and marine LiDAR data. *Molecular Ecology* **25:** 3845-3864.

Miller AD, Versace VL, Matthews TG, Montgomery S and Bowie KC (2013) Ocean currents influence the genetic structure of an intertidal mollusc in south-eastern Australia -

implications for predicting the movement of passive dispersers across a marine biogeographic barrier. *Ecology and Evolution* **3:** 1248-1261.

Miller DD, Ota Y, Sumaila UR, Cisneros-Montemayor AM and Cheung WWL (2018) Adaptation strategies to climate change in marine systems. *Global Change Biology* **24:** E1-E14.

Miller KJ, Maynard BT and Mundy CN (2009) Genetic diversity and gene flow in collapsed and healthy abalone fisheries. *Molecular Ecology* **18:** 200-211.

Miller KJ, Mundy CN and Mayfield S (2014) Molecular genetics to inform spatial management in benthic invertebrate fisheries: a case study using the Australian Greenlip Abalone. *Molecular Ecology* **23:** 4958-4975.

Morse ANC, Froyd CA and Morse DE (1984) Molecules from cyanobacteria and red algae that induce larval settlement and metamorphosis in the mollusk *Haliotis rufescens*. *Marine Biology* **81:** 293-298.

Nielsen EE, Hemmer-Hansen J, Poulsen NA, Loeschcke V, Moen T *et al.* (2009) Genomic signatures of local directional selection in a high gene flow marine organism; the Atlantic cod (*Gadus morhua*). *BMC Evolutionary Biology* **9:** 276.

Oksanen J, Blanchet FG, Kindt R, Legendre P, Minchin PR, *et al.* (2013) Package 'vegan'. Community ecology package, version, 2(9).

Peakall R, Smouse PE (2006) GENALEX 6: genetic analysis in Excel. Population genetics software for teaching and research. *Molecular Ecology Notes* **6:** 288–295.

Pearce A, Lenanton R, Jackson G, Moore J, Feng M *et al.* (2011) The "marine heat wave" off Western Australia during the summer of 2010/11, in *Fisheries Research Report No. 222*. Government of Western Australia, Department of Fisheries, Western Australia.

Petrik CM, Duffy-Anderson JT, Mueter F, Hedstrom K and Curchitser EN (2015) Biophysical transport model suggests climate variability determines distribution of Walleye Pollock early life stages in the eastern Bering Sea through effects on spawning. *Progress in Oceanography* **138:** 459-474.

Pfeifer SP, Laurent S, Sousa VC, Linnen CR, Foll M *et al.* (2018) The ecolutionary history of Nebraska deer mice: local adaptation in the face of strong gene flow. *Molecular Biology and Evolution* **35:** 792-806.

Pickrill RA, and Todd BJ (2003) The multiple roles of acoustic mapping in integrated ocean management, Canadian Atlantic continental margin. *Ocean & Coastal Management* **46:** 601-614.

Piggott MP, Banks SC, Tung P and Beheregaray LB (2008) Genetic evidence for different scales of connectivity in a marine mollusc. *Marine Ecology Progress Series* **365:** 127-136.

Plough LV (2012) Environmental stress increases selection against and dominance of deleterious mutations in inbred families of the Pacific oyster *Crassostrea gigas*. *Molecular Ecology* **21:** 3974-3987.

Plough LV, Shin G and Hedgecock D (2016) Genetic inviability is a major driver of type III survivorship in experimental families of a highly fecund marine bivalve. *Molecular Ecology* **25:** 895-910.

Postma FM, and Ågren J (2016) Early life stages contribute strongly to local adaptation in *Arabidopsis thaliana*. *Proceedings of the National Academy of Sciences* **113:** 7590-7595.

Price N, Moyers BT, Lopez L, Lasky JR, Monroe JG *et al.* (2018) Combining population genomics and fitness QTLs to identify the genetics of local adaptation in *Arabidopsis thaliana. Proceedings of the National Academy of Sciences of the United States of America* **115:** 5028-5033.

Prince JD, Sellers TL, Ford WB and Talbot SR (1987) Experimental evidence for limited dispersal of haliotid larvae (genus *Haliotis*; Mollusca: Gastropoda). *Journal of Experimental Marine Biology and Ecology* **106:** 243-263.

Prince JD, Sellers TL, Ford WB and Talbot SR (1988) Confirmation of a relationship between the localized abundance of breeding stock and recruitment for *Haliotis rubra* Leach (Mollusca: Gastropoda). *Journal of Experimental Marine Biology and Ecology* **122:** 91-104.

Raymond M, and Rousset F (1995) An exact test for population differentiation. *Evolution* **49:** 1280-1283.

Ridgway KR (2007) Long-term trend and decadal variability of the southward penetration of the East Australian Current. *Geophysical Research Letters* **34:** L13613.

Ridgway KR, and Condie SA (2004) The 5500-km-long boundary flow off western and southern Australia. *Journal of Geophysical Research-Oceans* **109:** 1-18.

Ridgway KR, and Godfrey JS (1997) Seasonal cycle of the East Australian Current. *Journal of Geophysical Research-Oceans* **102:** 22921-22936.

Roberts RD, Keys EF, Prendeville G and Pilditch CA (2007) Viability of abalone (*Haliotis iris*) stock enhancement by release of hatchery-reared seed in Marlborough, New Zealand. *Journal of Shellfish Research* **26:** 697-703.

Rodriguez SR, Ojeda FP and Inestrosa NC (1993) Settlement of benthic marine-invertebrates. *Marine Ecology Progress Series* **97:** 193-207.

Roodt-Wilding R (2007) Abalone ranching: a review on genetic considerations. *Aquaculture Research* **38:** 1229-1241.

Rousset F (1997) Genetic differentiation and estimation of gene flow from F-statistics under isolation by distance. *Genetics* **145:** 1219–1228.

1023 Sandery PA, and Kaempf J (2007) Transport timescales for identifying seasonal variation in Bass
1024 Strait, south-eastern Australia. *Estuarine Coastal and Shelf Science* **74:** 684-696.
1025 Sandoval-Castillo J, Robinson NA, Hart AM, Strain WS and Beheregaray LB (2018) Seascape
1026 genomics reveals adaptive divergence in a connected and commercially important mollusc,
1027 the greenlip abalone (*Haliotis laevigata*), along a longitudinal environmental gradient.
1028 *Molecular Ecology* **27:** 1603-1620.
1029 Sandoval-Castillo J, Strain WS, Hart AM, Robinson NA and Beheregaray LB (2015) Use of next
1030 generation DNA technologies for revealing the genetic impact of fisheries restocking and
1031 ranching, Adelaide: The Seafood CRC Company Ltd, the Fisheries Research and
1032 Development Corporation, Flinders University.
1033 Sappington JM, Longshore KM and Thompson DB (2007) Quantifying landscape ruggedness for
1034 animal habitat analysis: A case study using bighorn sheep in the Mojave Desert. *Journal of*
1035 *Wildlife Management* **71:** 1419-1426.
1036 Savolainen O, Lascoux M and Merila J (2013) Ecological genomics of local adaptation. *Nature*
1037 *Reviews Genetics* **14:** 807-820.
1038 Sherman, CDH, Ayre, DJ (2008) Fine-scale adaptation in a clonal sea anemone. *Evolution* **62:**
1039 1373-1380.
1040 Shiel BP, Hall NE, Cooke IR, Robinson NA and Strugnell JM (2015) De Novo
1041 Characterisation of the Greenlip Abalone Transcriptome (*Haliotis laevigata*) with a Focus
1042 on the Heat Shock Protein 70 (HSP70) Family. *Marine Biotechnology* **17:** 23-32.
1043 Sneed JM, Sharp KH, Ritchie KB and Paul VJ (2014) The chemical cue tetrabromopyrrole from a
1044 biofilm bacterium induces settlement of multiple Caribbean corals. *Proceedings of the Royal*
1045 *Society B-Biological Sciences* **281:** 1786.
1046 Solas MR, Sepulveda RD and Brante A (2013) Genetic variation of the shell morphology in
1047 *Acanthina monodon* (Gastropoda) in habitats with different wave exposure conditions.
1048 *Aquatic Biology* **18:** 253-260.
1049 Stapley J, Reger J, Feulner PGD, Smadja C, Galindo J *et al.* (2010) Adaptation genomics: the next
1050 generation. *Trends in Ecology & Evolution* **25:** 705-712.
1051 Takami H, Kawamura T and Yamashita Y (1997) Survival and growth rates of post-larval abalone
1052 *Haliotis discus hannai* fed conspecific trail mucus and/or benthic diatom *Cocconeis*
1053 *scutellum var. parva*. *Aquaculture* **152:** 129-138.
1054 Taniguchi IK, Stein D, Lampson K and Rogers-Bennett L (2013) Testing translocation as a
1055 recovery tool for pink (*Haliotis corrugata*) and green (*Haliotis fulgens*) abalone in southern
1056 California. *Journal of Shellfish Research* **32:** 209-216.

Temby N, Miller K and Mundy C (2007) Evidence of genetic subdivision among populations of blacklip abalone (*Haliotis rubra* Leach) in Tasmania. *Marine and Freshwater Research* **58:** 733-742.

Termignoni-Garcia F, Jaramillo-Correa JP, Chable-Santos J, Liu M, Shultz AJ *et al.* (2017) Genomic footprints of adaptation in a cooperatively breeding tropical bird across a vegetation gradient. *Molecular Ecology* **26:** 4483-4496.

Treml EA, Ford JR, Black KP and Swearer SE (2015) Identifying the key biophysical drivers, connectivity outcomes, and metapopulation consequences of larval dispersal in the sea. *Movement Ecology* **3**: 17.

Torda G, Donelson JM, Aranda M, Barshis DJ, Bay L *et al.* (2017) Rapid adaptive responses to climate change in corals. *Nature Climate Change* **7:** 627-636.

Twyford AD, and Friedman J (2015) Adaptive divergence in the monkey flower *Mimulus guttatu*s is maintained by a chromosomal inversion. *Evolution* **69:** 1476-1486.

van der Merwe M, Franchini P and Roodt-Wilding R (2011) Differential growth-related gene expression in abalone (*Haliotis midae*). *Marine Biotechnology* **13:** 1125-1139.

Walbridge S, Slocum N, Pobuda M, Wright DJ (208) Unified geomorphological analysis workflows with benthic terrain modeler. *Geosciences* **8:** 94.

Walker SJ (1999) Coupled hydrodynamic and transport models of Port Phillip Bay, a semi-enclosed bay in south-eastern Australia. *Marine and Freshwater Research* **50:** 469-481.

Waples RS (1998) Separating the wheat from the chaff: Patterns of genetic differentiation in high gene flow species. *Journal of Heredity* **89:** 438-450.

Waples RS, Punt AE and Cope JM (2008) Integrating genetic data into management of marine resources: how can we do it better? *Fish and Fisheries* **9:** 423-449.

Ward RD (2006) The importance of identifying spatial population structure in restocking and stock enhancement programmes. *Fisheries Research* **80:** 9-18.

Weeks AR, Heinze D, Perrin L, Stoklosa J, Hoffmann AA *et al.* (2017) Genetic rescue increases fitness and aids rapid recovery of an endangered marsupial population. *Nature Communications* **8:** 1071.

Weeks AR, Sgro CM, Young AG, Frankham R, Mitchell NJ *et al.* (2011) Assessing the benefits and risks of translocations in changing environments: a genetic perspective. *Evolutionary Applications* **4:** 709-725.

Weir B, and Cockerham C (1984) Estimating F-statistics for the analysis of population structure. *Evolution* **38:** 1358-1370.

Wernberg T, Russell BD, Moore PJ, Ling SD, Smale DA *et al.* (2011) Impacts of climate change in a global hotspot for temperate marine biodiversity and ocean warming. *Journal of Experimental Marine Biology and Ecology* **400:** 7-16.

Whiterod NS, Zukowski S, Asmus M, Gilligan D and Miller AD (2017) Genetic analyses reveal limited dispersal and recovery potential in the large freshwater crayfish Euastacus armatus from the southern Murray-Darling Basin. *Marine and Freshwater Research* **68:** 213-225.

Whitlock MC, and McCauley DE (1999) Indirect measures of gene flow and migration: F-ST not equal 1/(4Nm+1). *Heredity* **82:** 117-125.

Ye J, Fang L, Zheng HK, Zhang Y, Chen J *et al.* (2006) WEGO: a web tool for plotting GO annotations. *Nucleic Acids Research* **34:** W293-W297.

York KL, Blacket MJ and Appleton BR (2008) The Bassian Isthmus and the major ocean currents of southeast Australia influence the phylogeography and population structure of a southern Australian intertidal barnacle *Catomerus polymerus* (Darwin). *Molecular Ecology* **17:** 1948-1961.

Young IR, Zieger S and Babanin AV (2011) Global Trends in Wind Speed and Wave Height. *Science* **332:** 451-455.

Young M, Ierodiaconou D and Womersley T (2015) Forests of the sea: Predictive habitat modelling to assess the abundance of canopy forming kelp forests on temperate reefs. *Remote Sensing of Environment* **170:** 178-187.

Young MA, Iampietro PJ, Kvitek RG and Garza CD (2010) Multivariate bathymetry-derived generalized linear model accurately predicts rockfish distribution on Cordell Bank, California, USA. *Marine Ecology Progress Series* **415:** 247-261.

Young MA, Ierodiaconou D, Edmunds M, Hulands L and Schimel ACG (2016) Accounting for habitat and seafloor structure characteristics on southern rock lobster (*Jasus edwardsii*) assessment in a small marine reserve. *Marine Biology* **163:** 1-13.

Table 1 Site location details and corresponding codes for 29 collection sites of *Haliotis rubra* from south eastern Australia.

		GPS Location	
Zone and Location	Code	Latitude	Longitude
Western Zone			
Whites Beach	WHI	-38.349	141.384
Bully Cove	BUL	-38.397	141.411
Inside Murrels	INM	-38.404	141.526
Inside Nelson	INE	-38.404	141.560
Lawrence Rocks	LRO	-38.404	141.667
Lady Julia Percy Island	LJP	-38.421	141.995
The Craggs	OSC	-38.390	142.135
Warrnambool	WAR	-38.397	142.459
Central Zone			
Cat Reef	CAT	-38.741	143.188
Moonlight Head	MLH	-38.767	143.266
White Cliffs	WCF	-38.758	143.330
Blanket Bay	BLK	-38.827	143.586
Point Cook, Port Phillip Bay	PCO	-37.946	144.756
Freds Farm, Port Phillip Bay	FFM	-37.870	144.888
Seal Rocks	SRO	-38.528	145.100
The Nobbies	NOB	-38.518	145.110

Cape Woolami	WOO	-38.564	145.346
Arch Rock	ARK	-38.847	145.894
Cape Liptrap	LIP	-38.889	145.906
Cape Liptrap site 2	CCC	-38.901	145.913
Grinder Bay	GRB	-38.902	145.956
Tongue Point	TON	-38.994	146.258
Norman Point	NRM	-39.025	146.242
Great Glennie Island	GGI	-39.087	146.231
Norman Island	NMP	-39.053	146.320
Eastern Zone			
Marlo Frenches Narrows	MFN	-37.809	148.596
Point Ricardo	PRC	-37.813	148.619
Cape Conron	CCO	-37.814	148.731
East Cape Deep	ECD	-37.809	148.749

Table 2 Summary of environmental statistics for all 29 collection sites: geology, Vector Ruggedness Measure (VRM), average winter and summer wave power (kW/m); average winter and summer orbital velocity (m/s); average summer and seasonal range in sea surface temperature (^{O}C)

	Geology		Wave Power (kW/m)		Orbital Velocity (m/s)		Sea Surface Temperature (^{O}C)	
Code	Substrate	VRM	Winter	Summer	Winter	Summer	Summer	Seasonal Range
Western Zone								
WHI	Basalt	0.0017	8.20	4.42	173.13	126.85	17.14	3.08
BUL	Basalt	0.0028	17.64	10.54	177.84	135.03	17.93	3.07
INM	Calcareous	0.0007	6.51	4.96	189.12	160.40	17.96	3.55
INE	Calcareous	0.0007	5.87	3.89	84.83	63.09	17.96	3.55
LRO	Calcareous	0.0028	4.28	1.81	36.42	17.77	18.30	3.74
LJP	Basalt	0.0000	28.76	15.94	97.71	60.13	18.14	3.67
OSC	Basalt	0.0014	20.96	12.04	171.03	121.20	18.21	3.83

WAR	Calcareous	0.0037	3.31	2.24	56.00	44.62	18.07	3.97
Central Zone								
CAT	Calcareous	0.0049	20.66	12.86	206.55	159.15	17.69	3.41
MLH	Calcareous	0.0022	0.00	0.00	0.03	0.02	17.69	3.45
WCF	Calcareous	0.0015	14.52	8.96	168.51	123.96	17.65	3.47
BLK	Calcareous	0.0011	2.36	1.81	39.58	32.55	17.88	3.96
PCO	Basalt	0.0000	0.00	0.01	0.78	0.72	21.12	9.39
FFM	Basalt	0.0001	0.01	0.01	0.66	0.70	21.34	9.61
SRO	Basalt	0.0010	0.00	0.00	0.01	0.01	19.04	6.11
NOB	Basalt	0.0012	7.07	4.77	79.35	62.28	19.04	6.11
WOO	Granite	0.0034	8.82	5.62	22.65	13.86	19.05	5.52
ARK	Calcareous	0.0009	9.17	5.42	110.09	85.43	18.78	5.13
LIP	Calcareous	0.0018	9.58	5.29	107.92	77.24	18.78	5.13
CCC	Calcareous	0.0029	11.34	6.27	89.30	61.95	18.68	4.92
GRB	Granite	0.0019	4.46	3.12	107.46	87.20	18.68	4.92
TON	Granite	0.0008	7.01	3.77	42.15	29.24	18.58	4.99
NRM	Granite	0.0002	8.86	3.54	5.76	2.48	18.43	4.76
GGI	Granite	0.0005	9.85	4.93	4.46	2.08	18.15	4.49
NMP	Granite	0.0035	3.90	2.47	41.60	35.35	18.58	4.99
Eastern Zone								
MFN	Calcareous	0.0003	3.27	1.77	26.99	14.92	18.62	5.20
PRC	Calcareous	0.0003	3.15	1.75	25.07	14.19	18.62	5.20
CCO	Calcareous	0.0005	3.63	2.00	21.93	12.16	18.59	4.87
ECD	Calcareous	0.0005	3.65	2.00	33.98	20.03	18.59	4.87

Table 3 Numbers of candidate loci identified as having significant correlations with environmental covariables by BayPass, Latent Factor Mixed Modelling (LFMM) and Redundancy Analysis (RDA) from a total dataset of 5,239 SNPs for the blacklip abalone *Haliotis rubra*.

	BayPass			LFMM	RDA	
	3 < BF < 10	10 < BF < 20	BF > 20	q <0.001	a = 0.05	Total candidates
Geology	60	15	4	N/A	29	106
VRM	48	23	3	12	16	95
Winter wave power	46	12	6	25	11	97
Summer wave power	39	11	5	23	12	88
Winter orbital velocity	13	0	1	22	12	43
Summer orbital velocity	13	7	0	24	8	48
Summer average SST	268	270	120	60	47	718
Seasonal temp range	24	18	0	40	0	76

1172

Table 4 SNP loci identified by GDM analyses as explaining greater than 0% deviance for each environmental variable. Numbers of non-significant candidates for each data set were as follows: winter wave power = 88; summer wave power = 80; seasonal temperature range = 74; summer sea surface temperature = 705; winter orbital velocity = 39; summer orbital velocity = 43; VRM = 75.

Environmental variable	SNP locus	Deviance (%)		Environmental variable	SNP locus	Deviance (%)
Winter wave Power	29000_33	13.2		Summer wave power	10080_72	0.34
	93527_52	0.07			12085_77	17.68
	94891_79	13.47			12099_54	0.07
	31220_73	7.62			14150_22	24.21
	81807_43	0.77			29000_33	14.88
	11925_63	1.03			93527_52	0.1
	10080_72	0.32			22064_40	10.0
	5351_44	8.8			34419_52	8.4
	8277_7	5.96				
Seasonal temperature range	12934_28	0.28		Summer sea surface temperature	9325_22	2.48
	32210_29	0.19			9379_73	0.6
					10080_72	0.55
Winter orbital velocity	8277_7	1.59			12934_28	0.28
	6784_54	3.15			14745_47	1.23
	25404_6	16.9			15884_37	2.03
	30737_35	27.4			17019_41	1.01
					24395_36	0.01
Summer orbital velocity	5038_65	4.92			30165_46	3.14
	6784_54	3.43			34419_52	1.31
	30165_46	4.4			50488_50	0.31
	30737_35	0.19			2755_22	0.34
	25404_6	0.001			32754_60	0.19
VRM	2755_22	5.3				
	8277_7	6.71				

	9824_42	0.03				
	11778_32	7				
	12077_74	2.54				
	13056_29	3.07				
	15442_53	9.75				
	15487_52	18.96				
	22064_40	0.34				
	34419_52	3.43				
	24136_79	6.65				
	24692_77	1.52				
	35093_14	18.12				
	2834_53	15.07				
	4401_40	11.96				
	5356_71	5.04				
	13077_33	17.19				
	13824_41	5.70				
	16880_71	8.53				

1177

Table 1 Site location details and corresponding codes for 29 collection sites of Haliotis rubra from south eastern Australia.

		GPS Location	
Zone and Location	Code	Latitude	Longitude
Western Zone			
Whites Beach	WHI	-38.349	141.384
Bully Cove	BUL	-38.397	141.411
Inside Murrels	INM	-38.404	141.526
Inside Nelson	INE	-38.404	141.560
Lawrence Rocks	LRO	-38.404	141.667
Lady Julia Percy Island	LJP	-38.421	141.995
The Craggs	OSC	-38.390	142.135
Warrnambool	WAR	-38.397	142.459
Central Zone			
Cat Reef	CAT	-38.741	143.188
Moonlight Head	MLH	-38.767	143.266
White Cliffs	WCF	-38.758	143.330
Blanket Bay	BLK	-38.827	143.586
Point Cook, Port Phillip Bay	PCO	-37.946	144.756
Freds Farm, Port Phillip Bay	FFM	-37.870	144.888
Seal Rocks	SRO	-38.528	145.100
The Nobbies	NOB	-38.518	145.110
Cape Woolami	WOO	-38.564	145.346
Arch Rock	ARK	-38.847	145.894
Cape Liptrap	LIP	-38.889	145.906
Cape Liptrap site 2	CCC	-38.901	145.913
Grinder Bay	GRB	-38.902	145.956
Tongue Point	TON	-38.994	146.258
Norman Point	NRM	-39.025	146.242
Great Glennie Island	GGI	-39.087	146.231
Norman Island	NMP	-39.053	146.320

Eastern Zone			
Marlo Frenches Narrows	MFN	-37.809	148.596
Point Ricardo	PRC	-37.813	148.619
Cape Conron	CCO	-37.814	148.731
East Cape Deep	ECD	-37.809	148.749

Table 2 Summary of environmental statistics for all 29 collection sites: geology, Vector Ruggedness Measure (VRM), average winter and summer wave power (kW/m); average winter and summer orbital velocity (m/s); average summer and seasonal range in sea surface temperature (^{O}C)

	Geology		Wave Power (kW/m)		Orbital Velocity (m/s)		Sea Surface Temperature (^{O}C)	
Code	Substrate	VRM	Winter	Summer	Winter	Summer	Summer	Seasonal Range
Western Zone								
WHI	Basalt	0.0017	8.20	4.42	173.13	126.85	17.14	3.08
BUL	Basalt	0.0028	17.64	10.54	177.84	135.03	17.93	3.07
INM	Calcareous	0.0007	6.51	4.96	189.12	160.40	17.96	3.55
INE	Calcareous	0.0007	5.87	3.89	84.83	63.09	17.96	3.55
LRO	Calcareous	0.0028	4.28	1.81	36.42	17.77	18.30	3.74
LJP	Basalt	0.0000	28.76	15.94	97.71	60.13	18.14	3.67
OSC	Basalt	0.0014	20.96	12.04	171.03	121.20	18.21	3.83
WAR	Calcareous	0.0037	3.31	2.24	56.00	44.62	18.07	3.97
Central Zone								
CAT	Calcareous	0.0049	20.66	12.86	206.55	159.15	17.69	3.41
MLH	Calcareous	0.0022	0.00	0.00	0.03	0.02	17.69	3.45
WCF	Calcareous	0.0015	14.52	8.96	168.51	123.96	17.65	3.47
BLK	Calcareous	0.0011	2.36	1.81	39.58	32.55	17.88	3.96
PCO	Basalt	0.0000	0.00	0.01	0.78	0.72	21.12	9.39
FFM	Basalt	0.0001	0.01	0.01	0.66	0.70	21.34	9.61
SRO	Basalt	0.0010	0.00	0.00	0.01	0.01	19.04	6.11
NOB	Basalt	0.0012	7.07	4.77	79.35	62.28	19.04	6.11
WOO	Granite	0.0034	8.82	5.62	22.65	13.86	19.05	5.52
ARK	Calcareous	0.0009	9.17	5.42	110.09	85.43	18.78	5.13
LIP	Calcareous	0.0018	9.58	5.29	107.92	77.24	18.78	5.13
CCC	Calcareous	0.0029	11.34	6.27	89.30	61.95	18.68	4.92
GRB	Granite	0.0019	4.46	3.12	107.46	87.20	18.68	4.92
TON	Granite	0.0008	7.01	3.77	42.15	29.24	18.58	4.99
NRM	Granite	0.0002	8.86	3.54	5.76	2.48	18.43	4.76
GGI	Granite	0.0005	9.85	4.93	4.46	2.08	18.15	4.49
NMP	Granite	0.0035	3.90	2.47	41.60	35.35	18.58	4.99
Eastern Zone								

MFN	Calcareous	0.0003	3.27	1.77	26.99	14.92	18.62	5.20
PRC	Calcareous	0.0003	3.15	1.75	25.07	14.19	18.62	5.20
CCO	Calcareous	0.0005	3.63	2.00	21.93	12.16	18.59	4.87
ECD	Calcareous	0.0005	3.65	2.00	33.98	20.03	18.59	4.87

Table 3 Numbers of candidate loci identified as having significant correlations with environmental covariables by BayPass, Latent Factor Mixed Modelling (LFMM) and Redundancy Analysis (RDA) from a total dataset of 5,239 SNPs for the blacklip abalone Haliotis rubra.

	BayPass			LFMM	RDA	
	3 < BF < 10	10 < BF < 20	BF > 20	q <0.001	a = 0.05	Total candidates
Geology	60	15	4	N/A	29	106
VRM	48	23	3	12	16	95
Winter wave power	46	12	6	25	11	97
Summer wave power	39	11	5	23	12	88
Winter orbital velocity	13	0	1	22	12	43
Summer orbital velocity	13	7	0	24	8	48
Summer average SST	268	270	120	60	47	718
Seasonal temp range	24	18	0	40	0	76

Table 4 SNP loci identified by GDM analyses as explaining greater than 0% deviance for each environmental variable. Numbers of non-significant candidates for each data set were as follows: winter wave power = 88; summer wave power = 80; seasonal temperature range = 74; summer sea surface temperature = 705; winter orbital velocity = 39; summer orbital velocity = 43; VRM = 75.

Environmental variable	**SNP locus**	**Deviance (%)**		**Environmental variable**	**SNP locus**	**Deviance (%)**
Winter wave Power	29000_33	13.2		Summer wave power	10080_72	0.34
	93527_52	0.07			12085_77	17.68
	94891_79	13.47			12099_54	0.07
	31220_73	7.62			14150_22	24.21
	81807_43	0.77			29000_33	14.88
	11925_63	1.03			93527_52	0.1
	10080_72	0.32			22064_40	10.0
	5351_44	8.8			34419_52	8.4
	8277_7	5.96				
Seasonal temperature range	12934_28	0.28		Summer sea surface temperature	9325_22	2.48
	32210_29	0.19			9379_73	0.6
					10080_72	0.55
Winter orbital velocity	8277_7	1.59			12934_28	0.28
	6784_54	3.15			14745_47	1.23
	25404_6	16.9			15884_37	2.03
	30737_35	27.4			17019_41	1.01
					24395_36	0.01
Summer orbital velocity	5038_65	4.92			30165_46	3.14
	6784_54	3.43			34419_52	1.31
	30165_46	4.4			50488_50	0.31

	30737_35	0.19			2755_22	0.34
	25404_6	0.001			32754_60	0.19
VRM	2755_22	5.3				
	8277_7	6.71				
	9824_42	0.03				
	11778_32	7				
	12077_74	2.54				
	13056_29	3.07				
	15442_53	9.75				
	15487_52	18.96				
	22064_40	0.34				
	34419_52	3.43				
	24136_79	6.65				
	24692_77	1.52				
	35093_14	18.12				
	2834_53	15.07				
	4401_40	11.96				
	5356_71	5.04				
	13077_33	17.19				
	13824_41	5.70				
	16880_71	8.53				

mec_15128_f1.tif

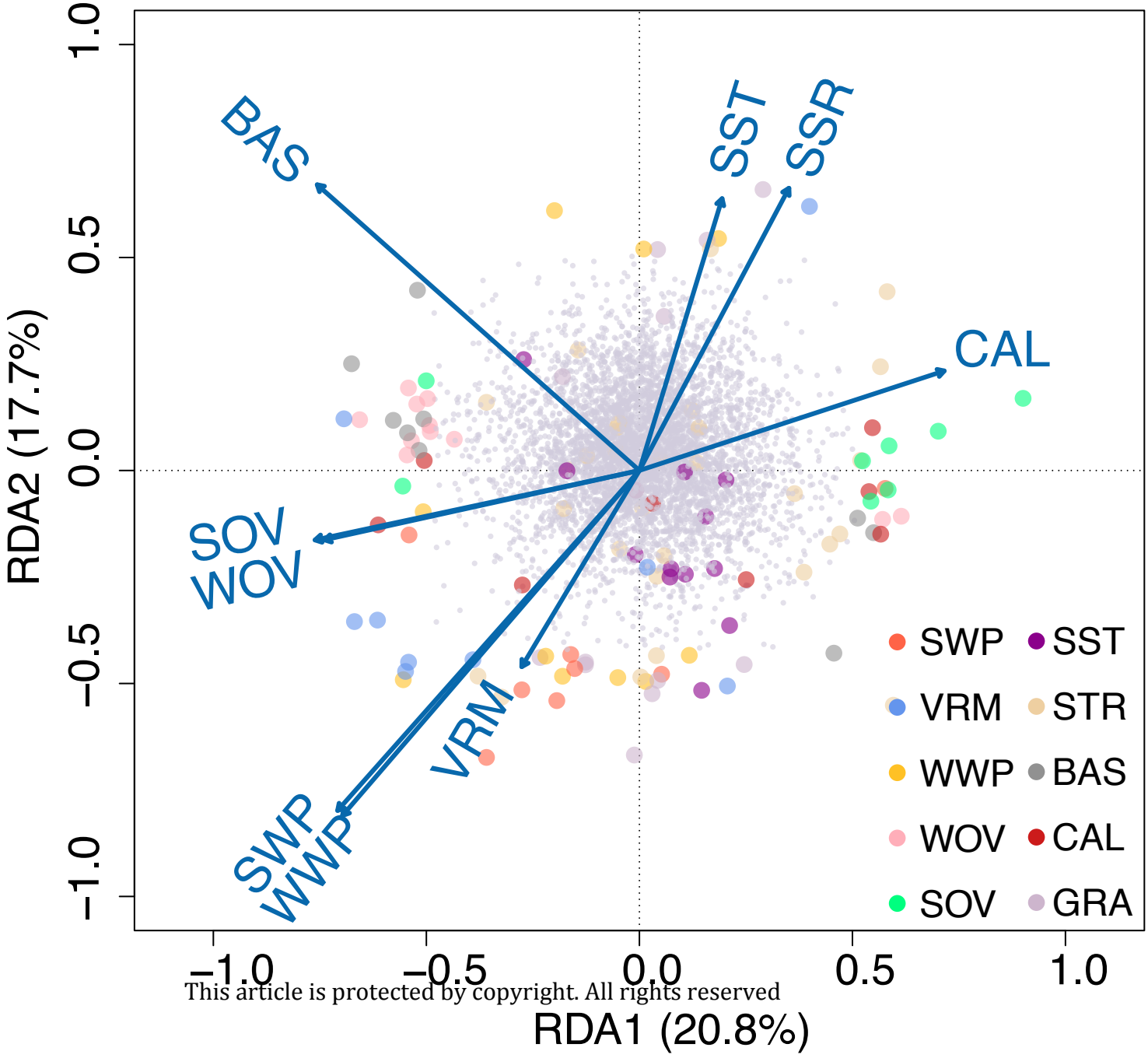

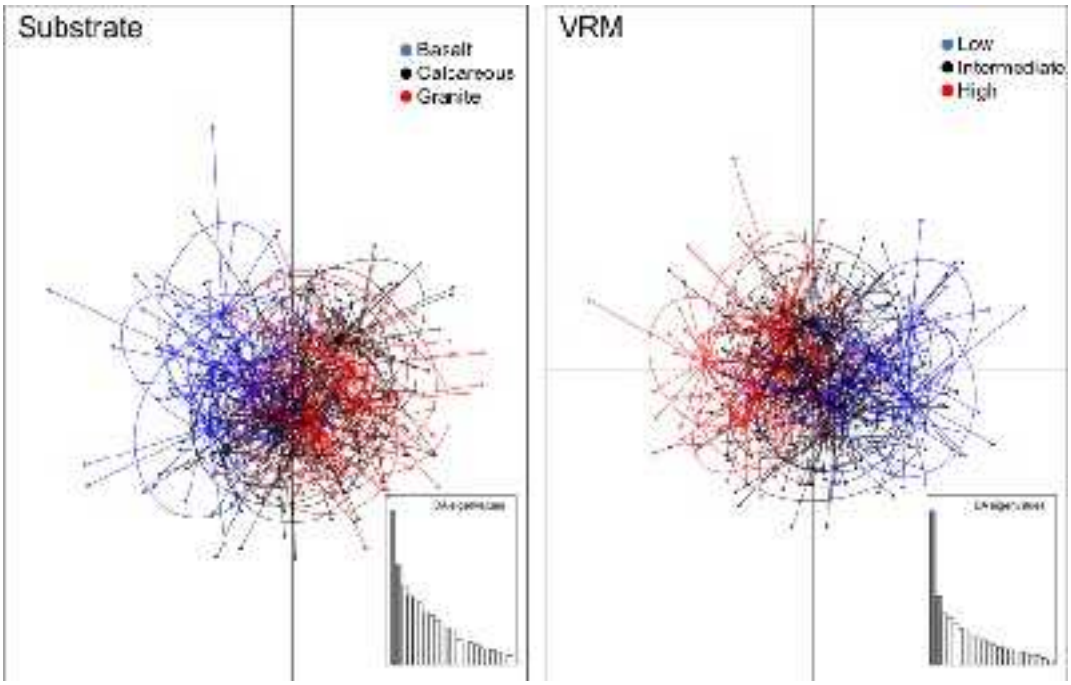

mec_15128_f3.png

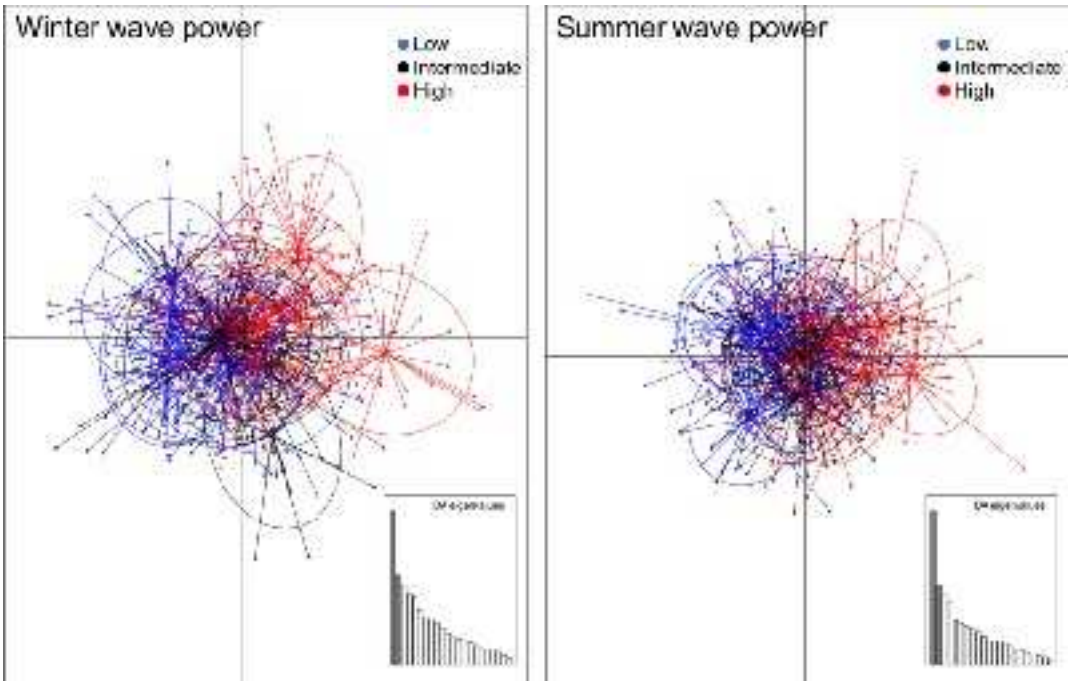

mec_15128_f4.png

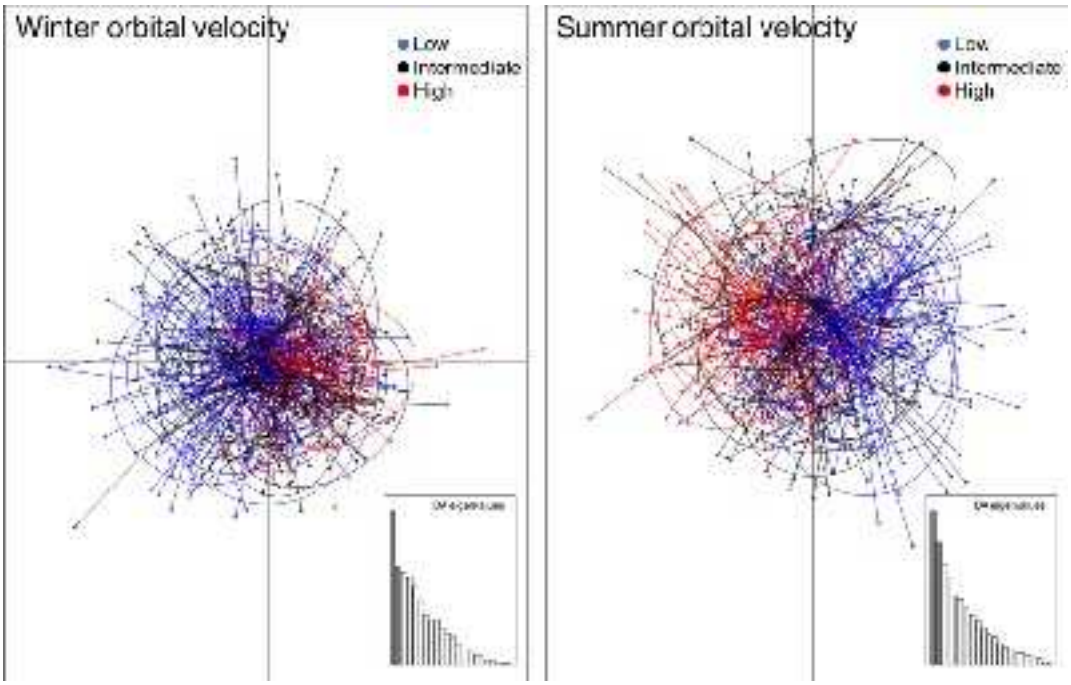

mec_15128_f5.png

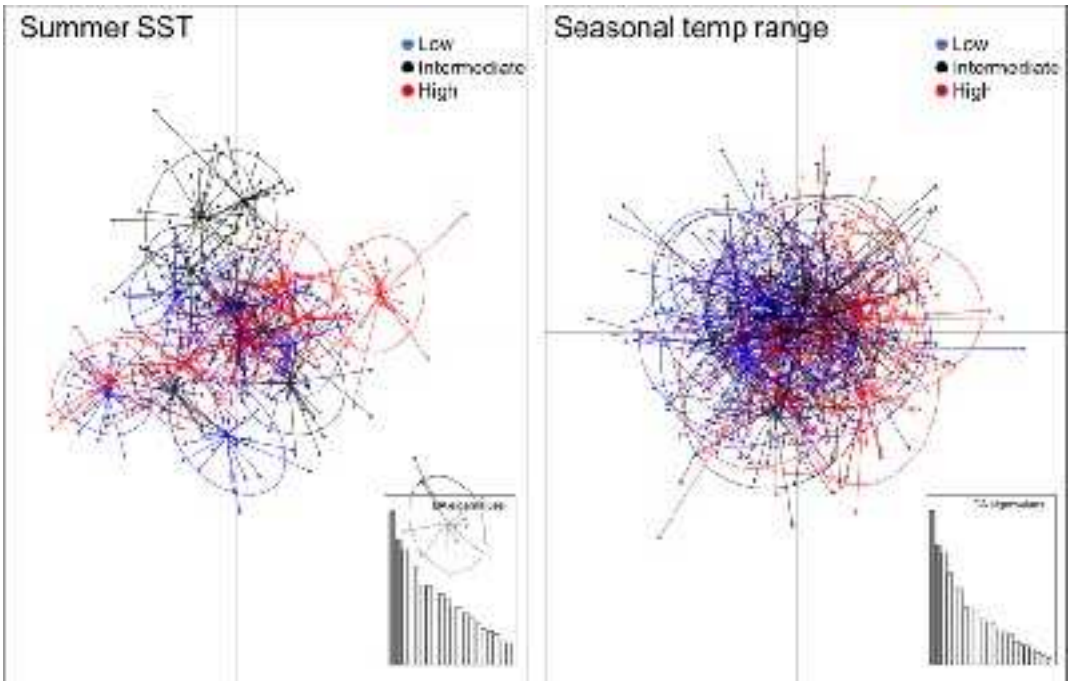

mec_15128_f6.png

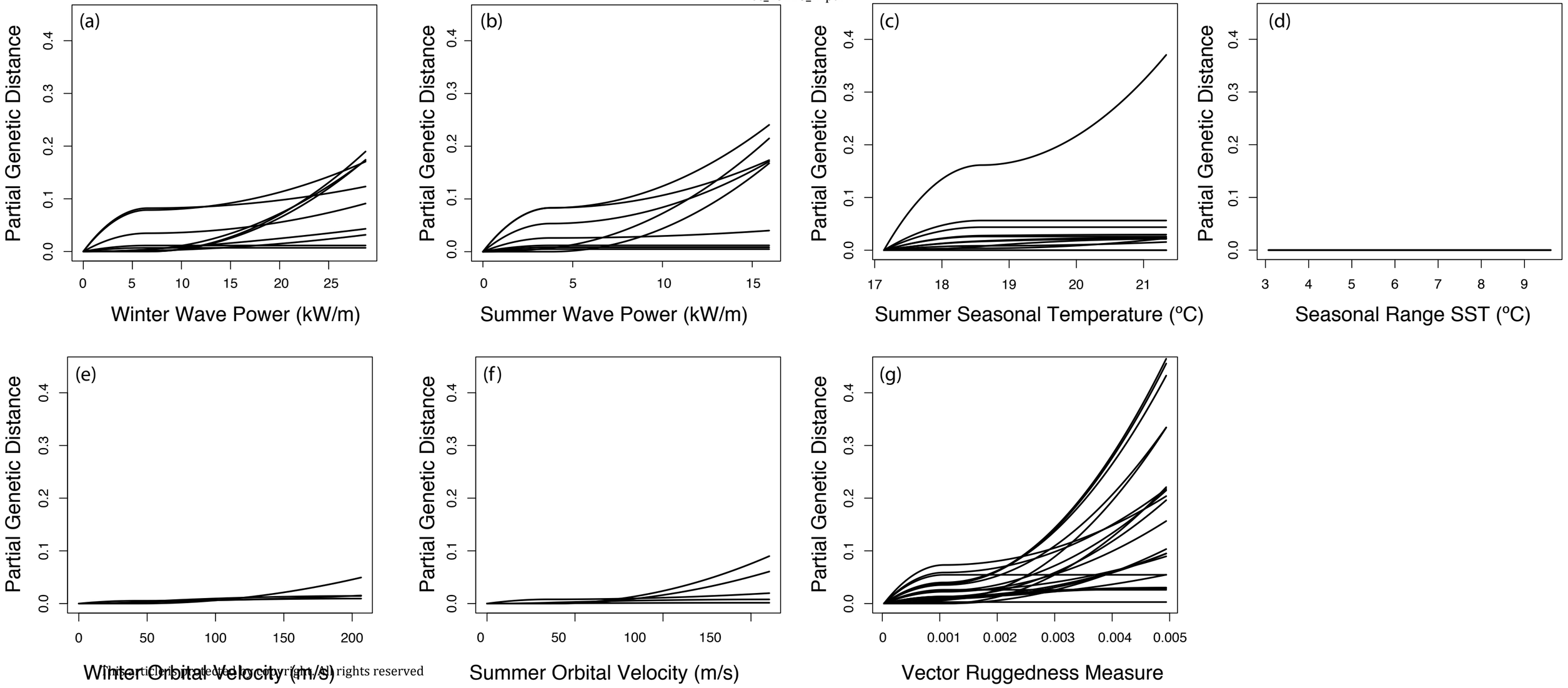

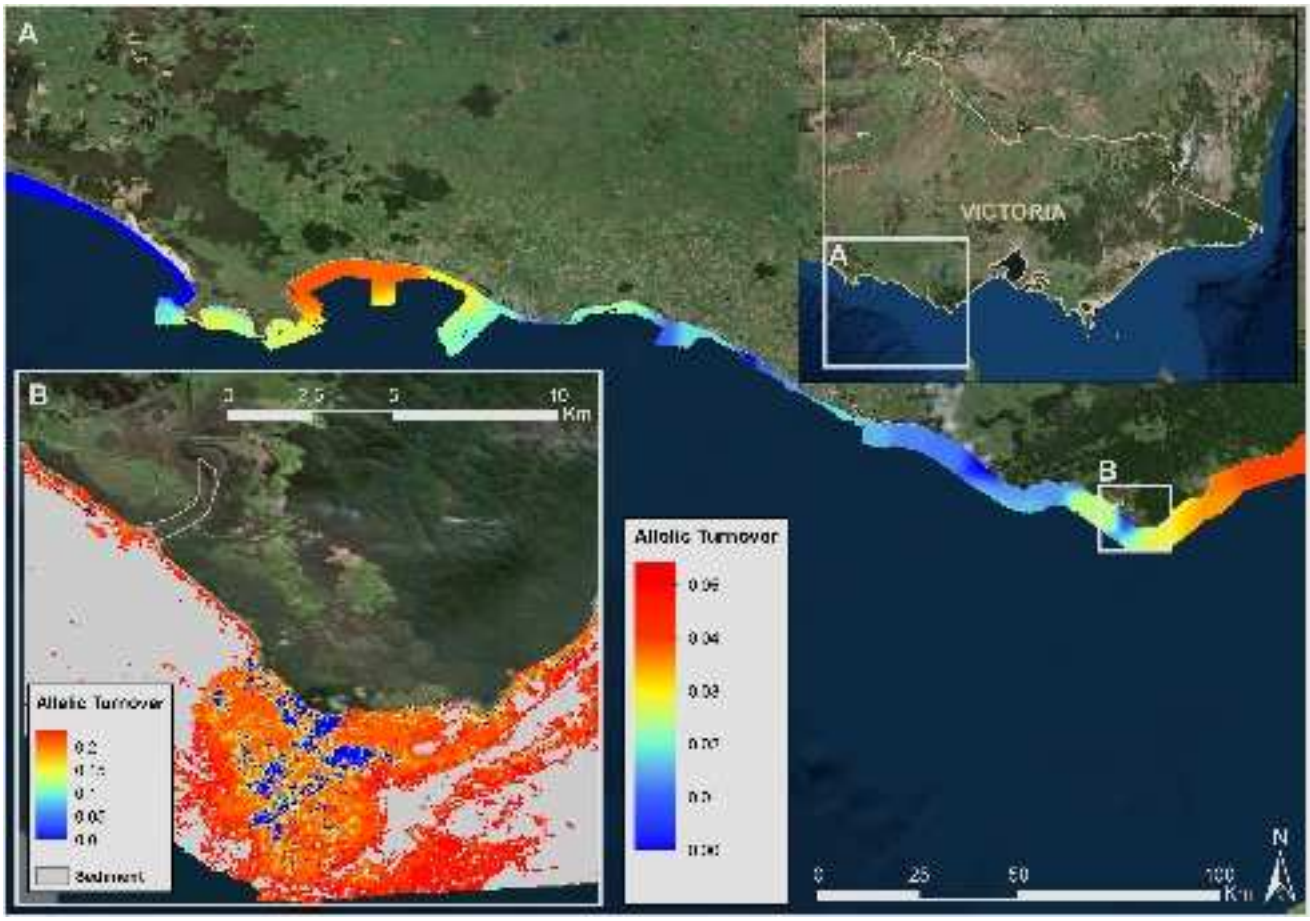

mec_15128_f8.tif